Reprinted from
Jpn J Clin Oncol 2005;35(6)338–341
doi:10.1093/jjco/hyi091

Surgery Including Liver Resection for Metastatic Gastrointestinal Stromal Tumors or Gastrointestinal Leiomyosarcomas

Souya Nunobe, Tsuyoshi Sano, Kazuaki Shimada, Yoshihiro Sakamoto and Tomoo Kosuge

Department of Surgery, National Cancer Center, Tokyo, Japan

Received January 7, 2005; accepted April 17, 2005; published online May 31, 2005

Jpn J Clin Oncol 2005;35(6)338–341
doi:10.1093/jjco/hyi091

Surgery Including Liver Resection for Metastatic Gastrointestinal Stromal Tumors or Gastrointestinal Leiomyosarcomas

Souya Nunobe, Tsuyoshi Sano, Kazuaki Shimada, Yoshihiro Sakamoto and Tomoo Kosuge

Department of Surgery, National Cancer Center, Tokyo, Japan

Received January 7, 2005; accepted April 17, 2005; published online May 31, 2005

Background: In recent years, imatinib mesylate (STI 571), a tyrosine kinase inhibitor, has shown short-term clinical usefulness for gastrointestinal stromal tumor or gastrointestinal leiomyosarcoma (GIST). The value of surgical resection, including hepatectomy, for metastatic GIST remains unknown. Our aim was to evaluate the outcome of surgical resection, including hepatectomy, for metastatic GIST at a single institute.
Methods: Eighteen patients who underwent hepatectomy for metastatic GIST were identified and the clinicopathological data of these patients were analyzed retrospectively.
Results: The primary site of GIST included stomach in 10, duodenum in five, ileum in two and esophagus in one patient. A hemihepatectomy or greater resection was undertaken in eight patients. Six patients underwent simultaneous resection for primary and hepatic desease. There was no in-hospital mortality in this series. The post-hepatectomy 3- and 5-year survival rates were 63.7 and 34.0% respectively, with a median of 36 (17–227) months. Recurrence after the initial hepatectomy was documented in 17 patients (94%), and metastatic mass of the remnant liver developed in 15 of these 17 patients (88%). Three patients survived >5 years after the initial hepatectomy who underwent multiple surgical resections during this period. No clinicopathological characteristic was a significant predictive factor for survival.
Conclusions: Multiple surgical resections, including hepatectomy, may contribute to important palliation in selected patients with metastatic GIST. Surgical cure seems to be difficult due to the high frequency of repeat metastasis to various sites. Therefore, adjuvant therapy must be required in the treatment of metastatic GIST.

Key words: gastrointestinal stromal tumor – liver metastasis – hepatectomy

INTRODUCTION

The liver is a common metastatic site for gastrointestinal stromal tumors or gastrointestinal leiomyosarcomas (GIST). Many patients with liver metastasis from GIST are either unresectable due to diffuse intrahepatic disease or inoperable due to extrahepatic disease. Some reports describing surgical resection of liver metastases from various sites of primary sarcoma have been published (1–3). In a recent analysis of 331 patients with liver metastasis from sarcoma, of which 131 patients had a GIST, 34 underwent hepatectomy of all gross disease (2). The post-operative 5-year survival rate was 30%, with a median survival of 39 months. The time interval from treatment of the primary tumor to the development of liver metastasis was a significant predictive factor of survival (2).

For reprints and all correspondence: Tsuyoshi Sano, Department of Surgery, National Cancer Center Central Hospital, 1-1 Tsukiji 5-chome, Chuo-ku, Tokyo 104-0045 Japan. E-mail: tsano@ncc.go.jp

Liver metastasis from GIST previously has been considered to be insensitive to chemotherapy or chemoembolization. Surgical resection is a possibly effective therapy and may provide a potential cure. However, imatinib mesylate (STI 571), currently being tested in clinical trials, has shown effectiveness for c-kit-positive GIST. STI 571 has demonstrated efficacy, minimal toxicity and a partial response rate of ~69% (4). Although there has been no complete response, the rate of disease progression has been only 11%. STI 571 has thus influenced the treatment of GIST patients dramatically.

This study reports the outcome of our 18 year experience at the National Cancer Center Central Hospital (NCCH) in Japan, to determine the value of surgical treatment, including hepatectomy, for patients with liver metastasis from GIST.

METHODS

From January 1984 to October 2003, there were 18 patients with liver metastasis from GIST who underwent hepatic resection of liver lesions with curative intent at the NCCH.

Patient demographics were recorded with the clinicopathological characteristics of the primary tumor and extent of intrahepatic and extrahepatic metastatic disease. Patients' date of treatment, recurrence and survival after hepatectomy were examined retrospectively in their medical records. The diagnosis of all liver metastases was confirmed by a pathologist at the NCCH. The long axis of the largest tumor was recorded as the tumor size. A synchronous metastasis was defined as the detection of a liver metastasis within 1 month of resection of the primary tumor.

Statistical analysis was performed with SPSS statistical softwear (Chicago, IL). Statistical significance was defined as $P < 0.05$. Cumulative survival was calculated using the Kaplan–Meier method. Univariate analysis was performed with Mann–Whitney U-test and log-rank test for survival.

RESULTS

Patient Characteristics

The clinicopathological variables of the patients with metastatic GIST to the liver are shown in Table 1. There were 10 (56%) males and eight (44%) females. The median age at diagnosis of the metastatic liver tumor was 58 years (range 33–65). There were 12 patients (67%) with metachronous liver lesions and six (33%) with synchronous lesions.

Tumor Characteristics

The distribution of primary tumor location included 10 cases in the stomach, five duodenal, two ileal and one in the esophagus. The size of the metastatic liver tumor was > 5 cm in 10 cases and ≤5 cm in eight cases (median 6.3 cm, range 1.6–24.0). Of 18 cases with hepatic metastases, 12 cases (67%) had multiple liver lesions. Five of these 12 cases had ≥5 liver lesions each. The time interval between the primary lesion and metastatic liver disease was ≥3 years in seven patients (median 53 months, 43–180), and <3 years in 11 patients including six patients with synchronous liver lesions (median 0 months, 0–35).

Treatment

Eight of 18 patients were treated with a lobectomy or greater resection, three with segmentectomies and seven with partial resection of the liver. Macroscopic complete resection of liver metastasis was achieved in 15 (83%) patients. No clinicopathological characteristic was a significant predictive factor for survival on univariate analysis (Table 1).

Survival and Recurrence

Of the 18 patients, 13 died from the primary disease, four were alive with disease, and only one was alive without recurrence, during a follow-up period of 35 months from the time of hepatic resection (Table 2). The median follow-up period after hepatectomy was 36 months (range 17–227). The post-hepatectomy 3- and 5-year survival rates were 63.7 and 34.0%, respectively (Fig. 1).

Recurrence following hepatectomy occurred in 17 patients (94%) including three patients who underwent macroscopic incomplete resection. The median time to first recurrence in those patients who underwent a macroscopic complete resection ($n = 15$) was 13.5 months (range 4–49). Fifteen patients (88%) developed recurrence within the remnant liver, of which six underwent a total of nine further hepatic resections (Table 2). Nine patients undertook other treatments for recurrent liver tumor including radiation in one, ethanol injection in two, radiofrequency ablation (RFA) in two, and chemotherapy in four including the use of STI 571 for three patients. Eleven patients (65%) developed recurrence within numerous other extrahepatic organs. Bone metastasis occurred in five patients, peritoneal disease in four and adrenal gland metastasis in two patients. Other metastatic sites included lung, chest

Table 1. Clinicopathological characteristics

			Median survival	
	n	%	Months	*P*-value
Gender				0.52
Female	8	44	38	
Male	10	56	38	
Age				0.62
≤50 years	7	39	40	
>50 years	11	61	38	
Primary site				0.75
Stomach	10	56	38	
Duodenum	5	28	37	
Ileum	2	11	23	
Esophagus	1	5	38	
Size of liver metastasis				0.36
≤5 cm	8	44	37	
>5 cm	10	56	38	
No. of liver metastases				0.88
Solitary	6	33	40	
Multiple	12	67	37	
Time to liver metastasis				
Synchronous	6	33	30	0.52
Metachronous	12	67	38	0.31
<3 years	11	61	34	
≥3 years	7	39	40	
Extent of hepatectomy				0.32
Less than lobectomy	10	56	40	
Lobectomy or more	8	44	34	
Radicality				0.48
Complete	15	83	38	
Incomplete	3	17	39	

wall, skin, soft tissue, brain and axillary lymph nodes. Six of these patients underwent a total of 18 further resections. Of these 17 patients with recurrent tumor after hepatectomy, nine cases (53%) had both intra- and extrahepatic recurrence.

Table 2. Survival and recurrence after hepatectomy

	n	%
Survival status		
No evidence of disease	1	5
Alive with disease	4	22
Died of disease	13	73
Recurrence in the remnant liver	15*	88
Resection	6	
Other treatment	9	
Recurrence of other site	11*	65
Resection	6	
Other treatment	5	

*Nine patients had both recurrence of remnant liver and extrahepatic organs.

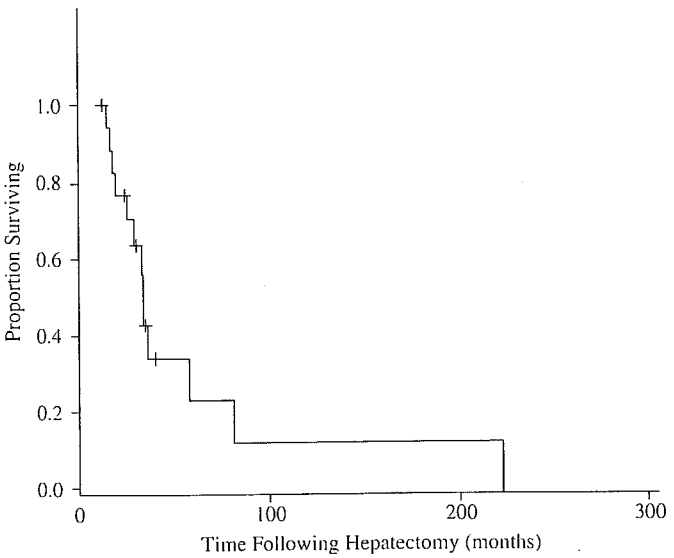

Figure 1. Survival after initial hepatectomy for metastases from GIST.

The initial hepatectomy resulted in macroscopic incomplete resection in three patients. One patient died of disease 19 months after hepatectomy. The other two patients were still alive at 39 and 45 months, receiving STI 571 administration following the hepatectomy.

Of all patients who underwent hepatectomy for liver metastasis from GIST, three patients survived >5 years after the initial hepatectomy (Table 3). Two of them underwent multiple resections for both recurrent extrahepatic disease and further hepatectomy for recurrent liver tumors. One patient underwent a total of 17 sessions of tumor resection: the liver twice, the chest wall twice, the lung four times, laminectomy twice and abdominal disease, left kidney and left iliac bone disease once each. The other patient underwent a total of five resections: the liver twice, the skin twice and soft tissue once. The time to recurrence after the initial hepatectomy in these three patients was 23, 35 and 49 months, respectively. This was a significantly longer interval compared with the remaining patients, excluding the three patients with incomplete initial hepatectomy (median 15 months, 4–24) ($P = 0.01$ using Mann–Whitney U-test).

DISCUSSION

Hepatectomy for metastasis from GIST has been reported previously (1–3), although the largest series included not only GIST but also soft tissue sarcoma or leiomyosarcoma. The post-operative 5-year survival rate in this patient group who underwent complete resection was 30%, with a median of 39 months (2). The present series focuses only on metastatic liver tumors from GIST, with an overall 5-year survival rate (including three patients with incomplete resection) of 34.0% and a median survival of 36 months, from the time of hepatic resection. This is similar to previously reported series. To know the natural history of the patient with metastatic GIST, it is crucial to evaluate the treatment strategy. However, as we had aggressively performed hepatectomy for metastatic GIST before the use of STI 571 was introduced, the clinical course of unresectable cases had not been followed in our institute. Therefore, we could not make a comparison between the treatment results of with/without hepatectomy. The reported response rates for chemotherapy of the tumor are poor, with a duration of response of only a few weeks or months (5,6).

Table 3. Five-year survivors after complete resection in three cases

Case	Age/sex	Primary site	Time of recurrence from hepatectomy	No of surgical inteventions		Status	Follow-up (months)
				Liver	Other site		
1	33/M	Ileum	49	3	9	DOD	227
2	63/F	Stomach	35	1	1	DOD	61
3	43/	Stomach	23	3	4	DOD	84

DOD, died of disease.

There were no other prognostic factors arising from the clinicopathological characteristics, including complete resection of all gross metastases, in the present series. Moreover, following hepatectomy for liver metastasis, there was a high proportion of recurrence in the remnant liver in addition to other organs. This result may show that surgical intervention for metastatic GIST is only palliative. However, three cases in our series had a long survival time of >5 years following repeated hepatectomy and tumor resection. In these three cases, the time to recurrence after the initial hepatectomy was statistically longer than that of the other patients. The longest survivor in our series was 227 months after the initial hepatectomy. Therefore, the only significant prognostic factor following hepatectomy on univariate analysis was a >5 year period to the development or recurrence (2). Other series have shown that metachronous metastases of ≥2 years from a complete resection of all gross disease was associated with a better prognosis on multivariate analysis. In all reports, the time to development of liver metastasis was invariantly an important prognostic factor in the surgical treatment. This time factor may be important in the selection of patients for treatment of recurrent tumor after hepatectomy.

Hepatectomy for potentially resectable metastatic colorectal tumor is now considered to be the first line therapy and its safety has been increasing, with an operative mortality and morbidity rate of 1.8 and 5%, respectively, in a recent large series (7). This series also reported a 5-year survival rate of up to 39%; other larger series have also reported much the same survival benefit (8). Overall, these data may imply that metastatic liver tumor from colorectal carcinoma via the portal venous system is not a reflection of systemic disease in the selected patients. In contrast, liver metastases from sarcomatous tumors reach the liver through the systemic circulation and therefore liver disease may merely reflect systemic disease. GIST are thought to be drained by portal vein blood flow as is the case in colorectal carcinoma. It may be important to determine the results of surgical treatment by focusing only on the liver metastasis from GIST. Unfortunately, the present study clearly reaffirms the difference between liver metastasis of GIST and colorectal carcinoma. The high rate of recurrence after hepatectomy for metastatic GIST implies that the disease had already become a systemic disease.

STI 571 is an inhibitor of the tyrosine kinase activity of c-kit and has shown good activity against GIST in clinical reports (4,9). It has been reported in a phase II trial that the partial response rate to STI 571 was 59% and that only 13% of 86 patients with GIST had progressive disease (10). However, in this trial, no complete response was obtained and therefore it is too early to confirm the duration of response in patients with STI 571-sensitive GIST. To test the benefit of adjuvant STI 571 in patients after complete resection of high-risk primary GIST, a phase II trial is being conducted by the American College of Surgeons Oncology Group (11). A prospective evaluation of neoadjuvant STI 571 therapy may be warranted. Two patients out of three in the present series, resulting from incomplete hepatectomy for metastatic GIST, received STI 571 for residual disease. They demonstrated a prolongation of survival, in keeping with a partial response.

Hepatectomy for metastatic GIST can be performed safely, and multiple surgical resections including hepatectomy may contribute to important palliation in selected patients with slow-growing metastatic GIST. However, surgical cure seems unlikely due to the high frequency of subclinical metastases, and hepatectomy may form only part of the therapy for metastatic GIST. Therefore, adjuvant therapy must be evaluated prospectively in the treatment of metastatic GIST.

Acknowledgments

This research was supported in part by a Grant-in-Aid for the Second Term Comprehensive 10-year Strategy for Cancer Control from the Ministry of Health, Labour and Welfare, Japan.

References

1. Lang H, Nußbaum KT, Kaudel P, Fruhauf N, Flemming P, Raab R. Hepatic metastases from leiomyosarcoma: a single-center experience with 34 liver resections during a 15-year period. *Ann Surg* 2000;231:500–5.
2. DeMatteo RP, Shah A, Fong Y. Results of hepatic resection for sarcoma metastatic to liver. *Ann Surg* 2001;234:540–8.
3. Elias D, Cavalcanti de Albuquerque A, Eggenspieler P, Plaud B, Ducreux M, Spielmann M, et al. Resection of liver metastases from a noncolorectal primary: indications and results based on 147 monocentric patients. *J Am Coll Surg* 1998;187:487–93.
4. van Oosterom AT, Judson I, Verweij J, Stroobants S, Donato di Paola E, Dimitrijevic S, et al. Safety and efficacy of imatinib (STI571) in metastatic gastrointestinal stromal tumors: a phase I study. *Lancet* 2001;358:1421–3.
5. Edmonson JH, Ryan LM, Blum RH, Brooks JS, Shiraki M, Frytak S, et al. Randomized comparison of doxorubicin alone versus ifosphamide or mitomycin, doxorubicin, and cisplatin against advanced soft tissue sarcomas. *J Clin Oncol* 1993;11:1269–75.
6. Casper ES, Christman KL, Schwartz GK, Johnson B, Brennan MF, Bertino JR. Edatrexate in patients with soft tissue sarcoma: activity in malignant fibrous histiocytoma. *Cancer* 1993;72:766–70.
7. Scheele J, Stang R, Altendorf-Hofmann A, Paul M. Resection of colorectal liver metastases. *World J Surg* 1995;19:59–71.
8. Fong Y, Fortner J, Sun RL, Brennan MF, Blumgart LH. Clinical score for predicting recurrence after hepatic resection for metastatic colorectal cancer: analysis of 1001 consecutive cases. *Ann Surg* 1999;230:309–21.
9. Joensuu H, Roberts PJ, Sarlomo-Rikala M, Andersson LC, Tervahartiala P, Tuveson D, et al. Effect of the tyrosine kinase inhibitor STI571 in a patient with a metastatic gastrointestinal stromal tumor. *N Engl J Med* 2001;344:1052–6.
10. Blanke CD, von Mehren M, Joensuu H, et al. Evaluation of the molecularly targeted therapy STI571 in patients with unresectable or metastatic gastrointestinal stromal tumors expressing KIT. *Proc Am Soc Clin Oncol* 2001;20:2.
11. American College of Surgeons Oncology Group. www.acosog.org 2001.

RNA Interference Targeting Aurora Kinase A Suppresses Tumor Growth and Enhances the Taxane Chemosensitivity in Human Pancreatic Cancer Cells

Tatsuo Hata,[1] Toru Furukawa,[1] Makoto Sunamura,[2] Shinichi Egawa,[2] Fuyuhiko Motoi,[2] Noriyuki Ohmura,[2] Tomotoshi Marumoto,[3] Hideyuki Saya,[3] and Akira Horii[1]

Departments of [1]Molecular Pathology and [2]Gastroenterological Surgery, Tohoku University School of Medicine, Sendai Miyagi, Japan and [3]Department of Tumor Genetics and Biology, Graduate School of Medical Sciences, Kumamoto University, Kumamoto, Japan

Abstract

***AURKA/STK15/BTAK*, the gene encoding Aurora A kinase that is involved in the regulation of centrosomes and segregation of chromosomes, is frequently amplified and overexpressed in various kinds of human cancers, including pancreatic cancer. To address its possibility as a therapeutic target for pancreatic cancer, we employed the RNA interference technique to knockdown *AURKA* expression and analyzed its phenotypes. We found that the specific knockdown of *AURKA* in cultured pancreatic cancer cells strongly suppressed *in vitro* cell growth and *in vivo* tumorigenicity. The knockdown induced the accumulation of cells in the G_2-M phase and eventual apoptosis. Furthermore, we observed a synergistic enhancement of the cytotoxicity of taxanes, a group of chemotherapeutic agents impairing G_2-M transition, by the RNA interference–mediated knockdown of *AURKA*. These results indicate that inhibition of *AURKA* expression can result in potent antitumor activity and chemosensitizing activity to taxanes in human pancreatic cancer.** (Cancer Res 2005; 65(7): 2899-905)

Introduction

Pancreatic cancer is one of the most common cancers with an extremely poor prognosis around the world because of its aggressive invasion, early metastasis, resistance to existing chemotherapeutic agents and radiation therapy, and lack of specific symptoms (1). To improve the horrible prognosis, we need to find novel approaches to both diagnosis and treatment that are far more efficient than currently available techniques. Molecular studies of cancers can lead us to find new drugs for molecular target therapy such as trastuzumab in breast cancer and gefitinib in lung cancer (2, 3). Pancreatic cancer involves very complicated molecular changes (4, 5); our previous comparative genomic hybridization analysis of the pancreatic cancer genome revealed intricate genomic alterations in multiple chromosome arms, including losses of 1p, 3p, 4q, 6q, 8p, 9p, 12q, 17p, 18q, and 21q and gains of 8q and 20q (6). The increase in copy number of 20q13 is especially prominent in pancreatic cancer (6, 7). Amplification of 20q13 is also found in several other types of human cancer such as colorectal cancer, breast cancer, bladder cancer, ovarian cancer, and hepatocellular cancer, suggesting the existence of an important oncogene(s) that plays a crucial role in a variety of human cancers in this area (8–12). *AURKA* was identified as one of the candidate oncogenes from the amplicon on 20q13 (13).

AURKA is one of three related genes (*AURKA*, *AURKB*, and *AURKC*) encoding AURORA kinases/serine-threonine kinases that play important roles in mitotic spindle formation and centrosome maturation and are physiologically essential for proper segregation of chromosomes into daughter cells (14). Since their discovery, the aurora kinases have been shown to be closely associated with carcinogenesis; an overexpression of AURKA transforms NIH3T3 cells and gives rise to aneuploid cells containing multiple centrosomes and multipolar spindles, indicating that *AURKA* is one of the fundamental cancer-associated genes and a potential target for diagnosis and treatment (14, 15). To further elucidate the possibility for utilization of *AURKA* in the treatment of human pancreatic cancer, we analyzed the phenotypes of cultured pancreatic cancer cells after RNA interference (RNAi)–mediated *AURKA* knockdown (16). Moreover, we tested the synergistic enhancement of the cytotoxicity of taxanes in pancreatic cancer cells by *AURKA*-RNAi.

Materials and Methods

Pancreatic cancer cell lines and cell culture. Three human pancreatic cancer cell lines, Panc-1, MIA PaCa-2, and SU.86.86, were purchased from American Type Culture Collection (Manassas, VA), and PK-1 was obtained from the original developer (17). All cells were maintained in RPMI 1640 containing 10% fetal bovine serum under atmosphere of 5% CO_2 with humidity at 37°C.

Short interference RNA transfection. Oligonucleotides of short interference double-strand RNAs (siRNA) with two thymidine residues (dTdT) overhanging at the 3′ end for knock down of the expressions of *AURKA* and the *luciferase* gene (*GL2*), including 5′-AUGCCCUGUCUUACUGUCA-3′ in the sense strand corresponding to nucleotides 725 to 743 relative to its start codon for the former (18) and 5′-CGUACGCGGAAUACUUCGA-3′ in the sense strand for the latter used as a control as described previously (19), were purchased from Japan Bioservice (Asaka, Japan). The siRNAs were dissolved into 5× annealing buffer [500 nmol/L potassium acetate, 150 nmol/L HEPES-KOH (pH 7.4), and 10 nmol/L magnesium acetate] to a final concentration of 20 μmol/L, boiled for 60 seconds, and gradually cooled down to 37°C for 60 minutes to anneal them. *In vitro* transfection was done using the Oligofectamine reagent (Invitrogen, Carlsbad, CA) according to the manufacturer's instructions.

Immunoblotting. A total of 3×10^5 cells were plated in 6-well plates (35 mm in diameter) and allowed to adhere for 24 hours; the transfection of double-stranded siRNA oligonucleotides was done as described above. After 48 hours, cells were harvested, and protein concentrations in total cell lysates were measured using the detergent-compatible protein assay kit (Bio-Rad, Hercules, CA). A 50-μg aliquot of the protein was subjected to immunoblotting as described previously using a 10% to 20% polyacrylamide gradient gel (Bio-Rad; ref. 20). The antibodies used were anti-AURKA

Requests for reprints: Akira Horii, Department of Molecular Pathology, Tohoku University School of Medicine, 2-1 Seiryo-machi, Aoba-ku, Sendai, 980-8575, Japan. Phone: 81-22-717-8042; Fax: 81-22-717-8047; E-mail: horii@mail.tains.tohoku.ac.jp.

polyclonal antibody (Transgenic, Kumamoto, Japan), anti-β actin monoclonal antibody (Sigma, St Louis, MO), and horseradish peroxidase–conjugated anti-mouse or anti-rabbit immunoglobulin antibodies (Amersham Biosciences Co., Piscataway, NJ). For blocking conditions and concentrations of antibodies, we followed the manufacturer's recommendations. Signals were visualized by reaction with enhanced chemiluminescence Detection Reagent (Amersham Biosiences) and digitally processed using LAS 1000 Plus with a Science Lab 99 Image Gauge (Fuji Photo Film, Minamiashigara, Japan).

3-(4,5-Dimethyl-2-thiazolyl)-2,5-diphenyl-2H-tetrazolium bromide assay. A total of 5×10^3 cells in 100 μL of the medium were plated in 96-well plates, and the RNA oligonucleotides were transfected. Every 24 hours up to 7 days, the medium was replaced with 100 μL of 0.05% 3-[4,5-dimethyl-2-thiazolyl]-2,5-diphenyl-2H-tetrazolium bromide (MTT)/PBS (−) and incubated for 1 hour. After the incubation, the MTT solution was removed, and the cells were suspended in 100% ethanol. Absorbance was measured at 590 nm using Versamax microplate reader (Amersham Biosiences).

Flowcytometry. Cells were harvested with trypsin-EDTA, washed with PBS (−), and fixed with 70% ethanol at −20°C for a few days. The fixed cells were pelleted, resuspended in 100 μL of hypotonic citric buffer (192 mmol/L Na_2HPO_4 and 4 mmol/L citric acid), and incubated for 30 minutes at room temperature. The cells were pelleted and suspended in PI/RNase/PBS (100 μg/mL propidium iodide and 10 μg/mL RNase A) overnight at 4°C. Analysis of DNA content was done on a FACSCalibur system (BD Immunocytometry Systems, San Jose, CA).

Plasmid constructions and colony formation assay. pSUPER-retro.-neo+GFP (pSR) vectors (ref. 21; Oligoengine, Seattle, WA) harboring gatccccATGCCCTGTCTTACTGTCAttcaagagaTGACAGTAAGACAGGGCATttttta and gatccccCGTACGCGGAATACTTCGAttcaagagaTCGAAGTATTCCGCGTACGttttta at its *Bgl*II/*Hin*dIII sites were prepared for expressing short hairpin RNAs (shRNA), as indicated in upper cases, specific for interfering expressions of *AURKA* (pSR-shAURKA) and *luciferase* (pSR-shGL2), respectively. The fidelity of the inserts was confirmed by sequencing both strands with primers of 5′-CGATCCTCCCTTTATCCAGC-3′ for the sense strand and 5′-CAGAACACATAGCGACATGC-3′ for the antisense strand using an ABI PRIZM BigDye Terminator Cycle Sequencing FS Ready Reaction Kit and an ABI PRIZM 310 DNA Analyzer according to the manufacturer's instructions (Applied Biosystems, Foster City, CA). For colony formation assays, 1×10^6 cells were plated in 10-cm culture dishes and transfected with 4 μg of either pSR-shAURKA, pSR-shGL2, or pSR using LipofectAMINE PLUS reagent (Invitrogen) according to the manufacturer's protocol. After 24 hours, transfected cells were passaged and cultured in the appropriate culture medium containing G418 at 500 μg/mL in concentration. After 14 days, cells were fixed with methanol and stained with 0.1% crystal violet. Visible colonies were manually counted.

Tumorigenicity in mice xenograft model. Four-week-old female Crj:CD-1(ICR)-nu mice were obtained from Charles River Japan, Inc. (Yokohama, Japan) and maintained under pathogen-free conditions. Each aliquot of 2×10^6 cells of MIA PaCa-2 stably trasfected with either pSR-shAURKA or pSR-shGL2 was suspended into 100 μL of PBS (−) containing 20% of Matrigel Growth Factor Reduced (Becton Dickinson Labware, Flanklin, NJ). These two sets of cells were s.c. injected into both flanks of mice. The inoculations were done in six mice. Tumor diameters were measured every 3 days, and each tumor volume in mm^3 was calculated by the following formula: $V = 0.4 \times D \times d^2$ (V, volume; D, longitudinal diameter; d, latitudinal diameter). Animal experiments in this study were done in compliance with Tohoku University School of Medicine institutional guidelines.

Statistical analysis. All experiments were done in duplicate or triplicate. A two-tailed Student's t test was used for statistical analysis of comparative data using Microsoft Excel software (Microsoft Co., Tokyo, Japan). Values of $P < 0.05$ were considered as significant and indicated by asterisks in the figures.

Results

Specific knockdown of *AURKA* in pancreatic cancer cell lines. To address the question of whether AURKA could serve as a therapeutic target for pancreatic cancer, we employed the siRNA method in an attempt to deplete the expression of AURKA in cultured pancreatic cancer cells. We prepared 21-mer oligoribonucleotides targeting *AURKA* and *Photinus pyralis luciferase* (*GL2*) based on information described elsewhere (18, 19). The oligoribonucleotides were annealed to give a double-strand siRNA and were transfected at 200 nmol/L into pancreatic cancer cells, MIA PaCa-2, Panc-1, PK-1, and SU.86.86, using the Oligofectamine reagent. After 48 hours, the cells were harvested, and their total lysates were analyzed by immunoblotting to see the effects of the siRNA on AURKA protein levels. As shown in Fig. 1*A*, dramatic suppression of

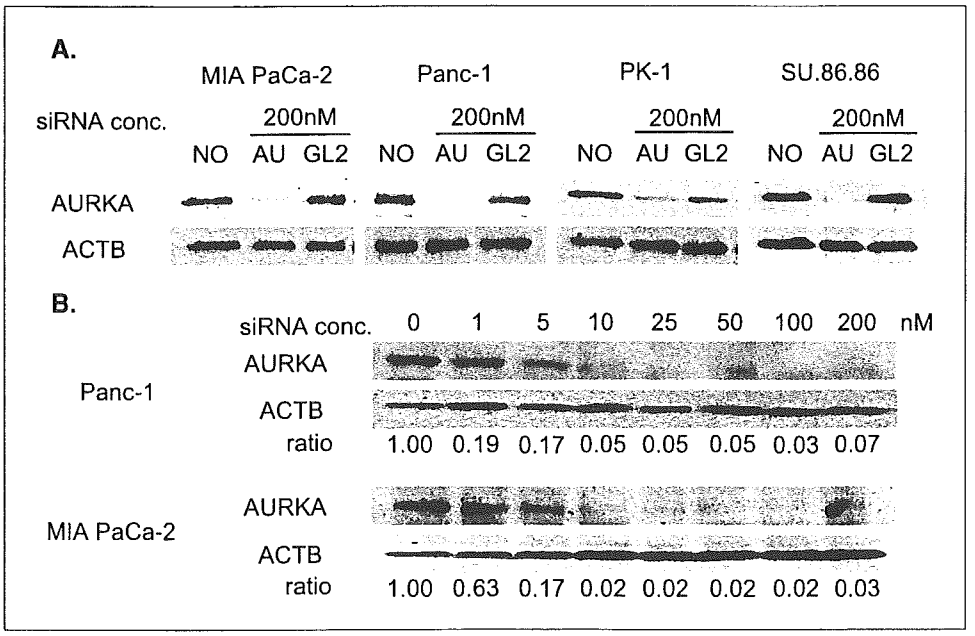

Figure 1. siRNA directed against *AURKA* specifically inhibits its expression. *A*, expression of *AURKA* 48 hours after the transfection of siRNA at 200 nmol/L directed against *AURKA* (*AU*) and *luciferase* (*GL2*) in pancreatic cancer cell lines, MIA PaCa-2, Panc-1, PK-1, and SU.86.86, detected by immunoblotting. *NO*, no transfection. *B*, a dose-dependent knockdown of AURKA expression by siRNA. Panc-1 and MIA PaCa-2 cells were transfected with the siRNA targeting *AURKA* at various concentrations ranging from 0 to 200 nmol/L. Expression of AURKA 48 hours after the transfection was detected by immunoblotting. β-Actin expression was monitored as the control. The ratio of AURKA/β-actin was calculated by using densitometry, and values were normalized by dividing by the ratio at no treatment (0 nmol/L).

AURKA expression was observed in all four cell lines by the siRNA targeting *AURKA* but not *GL2*. The siRNA oligonucleotides did not cause a nonspecific inhibition of gene expression, as shown by expressions of β-actin. Furthermore, the suppression of AURKA protein levels was achieved in a dose-dependent manner as shown in Fig. 1*B*; partial to complete suppressions were observed along with increasing concentrations of the siRNA oligonucleotides.

Knockdown of *AURKA* inhibits *in vitro* growth and colony formation. In phenotypic analyses, we first investigated effects of *AURKA* siRNA on the *in vitro* growth of pancreatic cancer cells. The siRNA transfection was done at 200 nmol/L to achieve complete suppression of AURKA expression, and cellular proliferations were monitored by MTT assay daily for 7 days. As shown in Fig. 2*A*, cell proliferation was significantly suppressed by *AURKA*-siRNA in all four pancreatic cancer cell lines as compared with *GL2*-siRNA. To observe the stable phenotypic consequences of siRNA-mediated knockdown in the cells, the 19-mer target sequences bridged by a 9-mer spacer were introduced into the

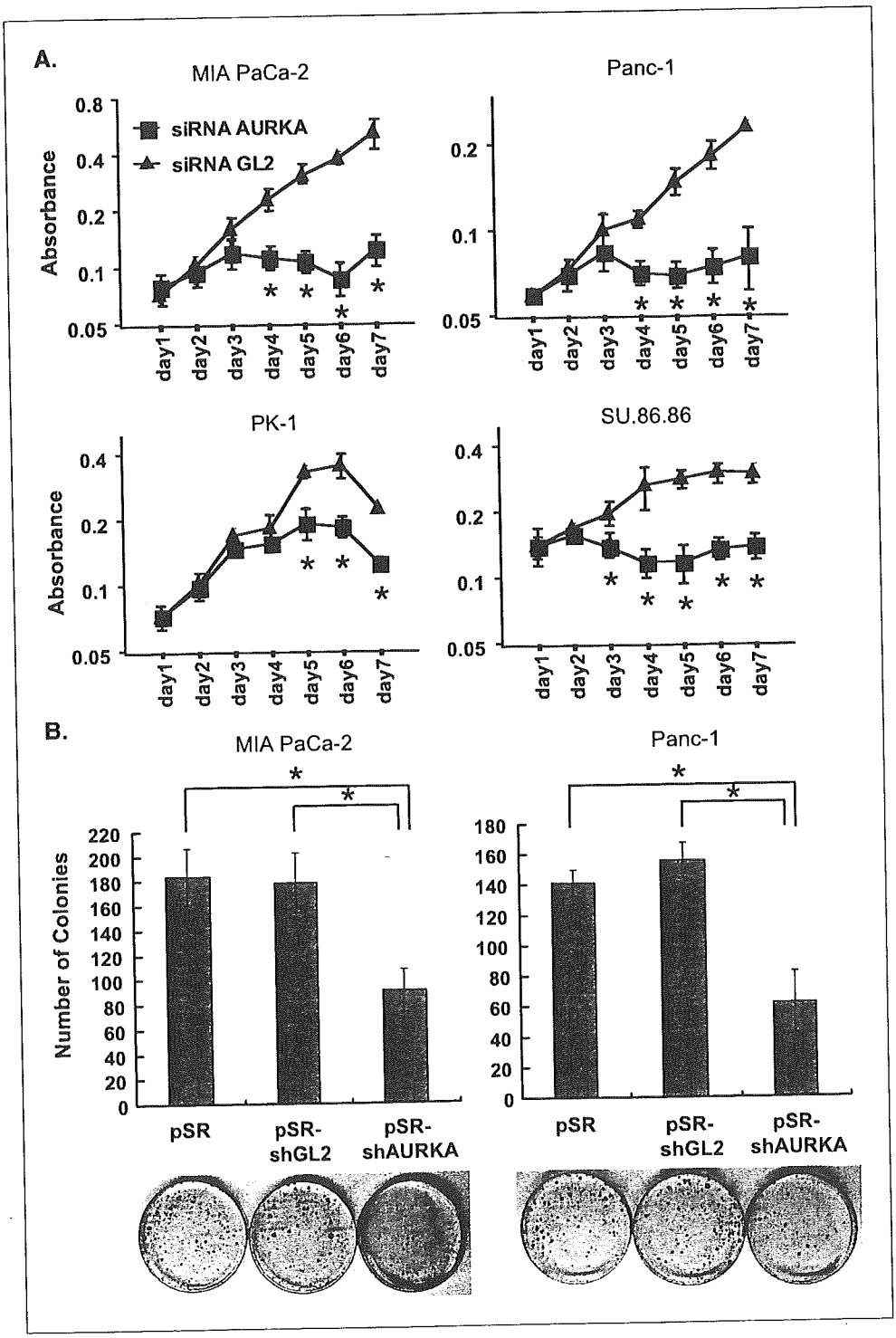

Figure 2. siRNA directed against *AURKA* suppresses *in vitro* growth of the pancreatic cancer cells. *A*, MTT assay of *in vitro* proliferation of the cells. These experiments were performed for four times. *B*, colony formation assay of G418-resistant colonies of the cells transfected either with pSUPER.retro.neo+GFP vector (pSR), pSR expressing short hairpin RNA directed against *AURKA* (pSR-shAURKA) or that directed against *luciferase* (pSR-shGL2). These experiments were performed for four times. *, $P < 0.05$.

pSUPER.retro.neo+GFP (pSR) vector to generate a short hairpin RNA targeting *AURKA* (pSR-shAURKA) or *luciferase* (pSR-shGL2), as described in Materials and Methods. For the colony formation assay using these vectors, MIA PaCa-2 and Panc-1 cells were transfected with either pSR-shAURKA, pSR-shGL2, or pSR empty vector and maintained in the selection medium containing G418 for 2 weeks. As expected from the MTT assay done in the siRNA experiment, the numbers of colonies were significantly decreased in pSR-shAURKA transfectants compared with the controls in both cell lines (see Fig. 2*B*). These results indicated that the RNAi-mediated specific knockdown of *AURKA* induced strong inhibition of pancreatic cancer cell growth *in vitro*.

Knockdown of *AURKA* suppresses tumorigenicity *in vivo*. We wondered whether the down-regulation of *AURKA* expression in pancreatic cancer cells would affect their ability to form tumors in nude mice. To address this question, we established stable transfectants of MIA PaCa-2 cells with treatment by either pSR-shAURKA or pSR-shGL2. These cells had modestly reduced expression of the AURKA protein (Fig. 3*A*). We then tested the *in vitro* growth of these cells and found that they showed rational growth retardation but not complete suppression, probably because of their modest level of knockdown of *AURKA* expression (Fig. 3*B*). Next, we injected the aliquot of 2×10^6 cells s.c. into six athymic nude mice and monitored their tumor growth. As shown in Fig. 3*C*, the pSR-shGL2 transfected cells gave rise to tumors within 4 weeks in all six mice, whereas the pSR-shAURKA transfected cells did not develop tumors in any of them. These results indicated that RNAi-mediated knockdown of *AURKA* exerted a strong antitumorigenic effect *in vivo* on pancreatic cancer cells.

Knockdown of *AURKA* induces G_2-M accumulation and apoptosis. AURKA is an important regulator of bipolar spindle formation and therefore essential for accurate chromosome segregation. We hypothesized that the growth suppression of the pancreatic cancer cells we observed by the RNAi-mediated knockdown of *AURKA* was caused by disruption of cell cycle transition with delay in mitotic entry, which has been shown in other kinds of mammalian cells (19, 22). To determine this possibility, we analyzed the DNA contents of cell populations reflecting the cell cycle distribution after knockdown of *AURKA* mediated by transfection of the siRNA in 200 nmol/L in MIA PaCa-2 and Panc-1 cells. As shown in Fig. 4*A*, an increase in the G_2-M population with a concomitant decrease in the G_0-G_1 population was observed after *AURKA*-siRNA treatment in both cells. Moreover, as we observed the changes in the DNA content during the time course after the transfection, we found obvious and significant increases in the sub-G_1 populations after 72 hours in MIA PaCa-2 cells and after 96 hours in Panc-1 cells (see Fig. 4*B*). These results indicate that the siRNA-mediated knockdown of *AURKA* led the pancreatic cancer cells to abnormal accumulation in the G_2-M phase and to eventual apoptosis.

Knockdown of *AURKA* significantly enhances cytotoxicities of taxanes. Taxanes, chemotherapeutic agents impairing the disassembly of microtubules that is crucial for the proper segregation of chromosomes during mitosis of eukaryotic cells, may synergistically enhance the effect of RNAi-mediated knockdown of *AURKA*, because it can accumulate cells in the G_2-M phase where AURKA plays essential roles. To determine this possibility, we investigated the synergistic effects of *AURKA* siRNA and taxanes in MIA PaCa-2 and Panc-1 cells. First, we searched for the best concentration of siRNAs in this experiment because siRNA treatment itself showed some cytotoxicities. The concentration at 10 nmol/L seemed to be the best because no significant difference in cell proliferation between *AURKA*-siRNA and *GL2*-siRNA treatments was found (data not shown). The concentration for paclitaxel and docetaxel were set by IC_{50} previously determined by MTT assay (data not shown). Then we

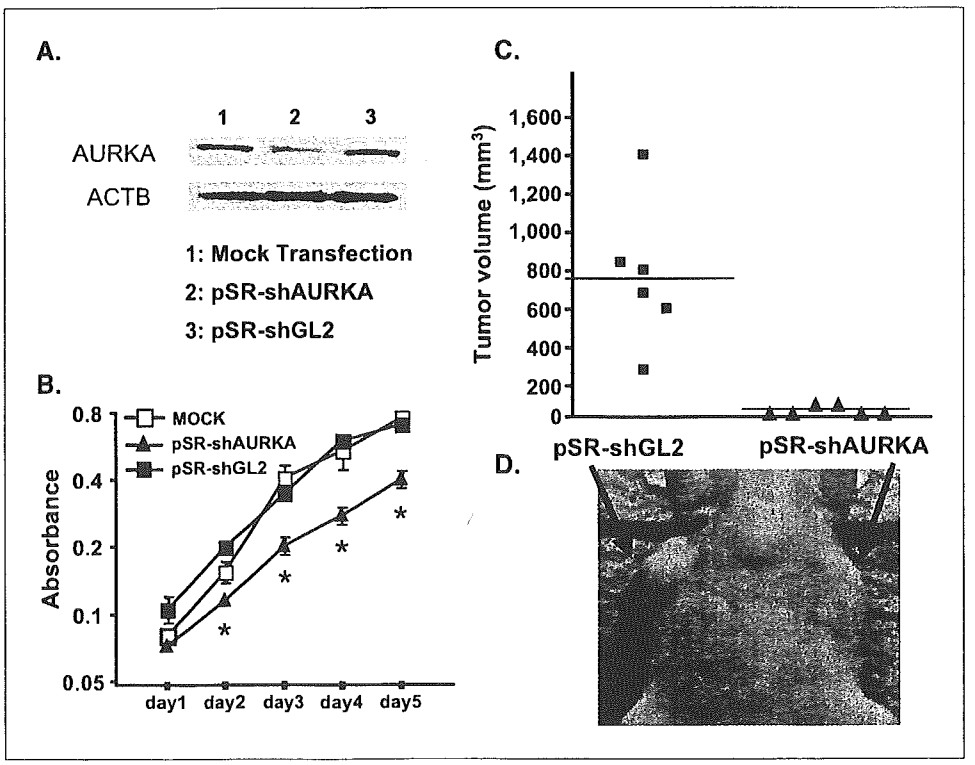

Figure 3. Stable suppression of *AURKA* inhibits *in vivo* tumorigenicity. *A*, *AURKA* expressions in MIA PaCa-2 cells stably transfected with pSR-shAURKA or pSR-GL2. *Mock*, no transfection. *B*, MTT assay of *in vitro* growth of the stable clones. These experiments were performed for four times. *, $P < 0.05$ (significant differences between mock and pSR-shAURKA and between pSR-shGL2 and pSR-shAURKA). *C*, tumorigenicity of the stable clones in the mouse-xenografted model. The stable clones were inoculated s.c. into both flanks of six nude mice. Sizes of the tumors generated were measured at 4 weeks after the inoculation. *D*, representative features of tumors in a mouse 4 weeks after the inoculation.

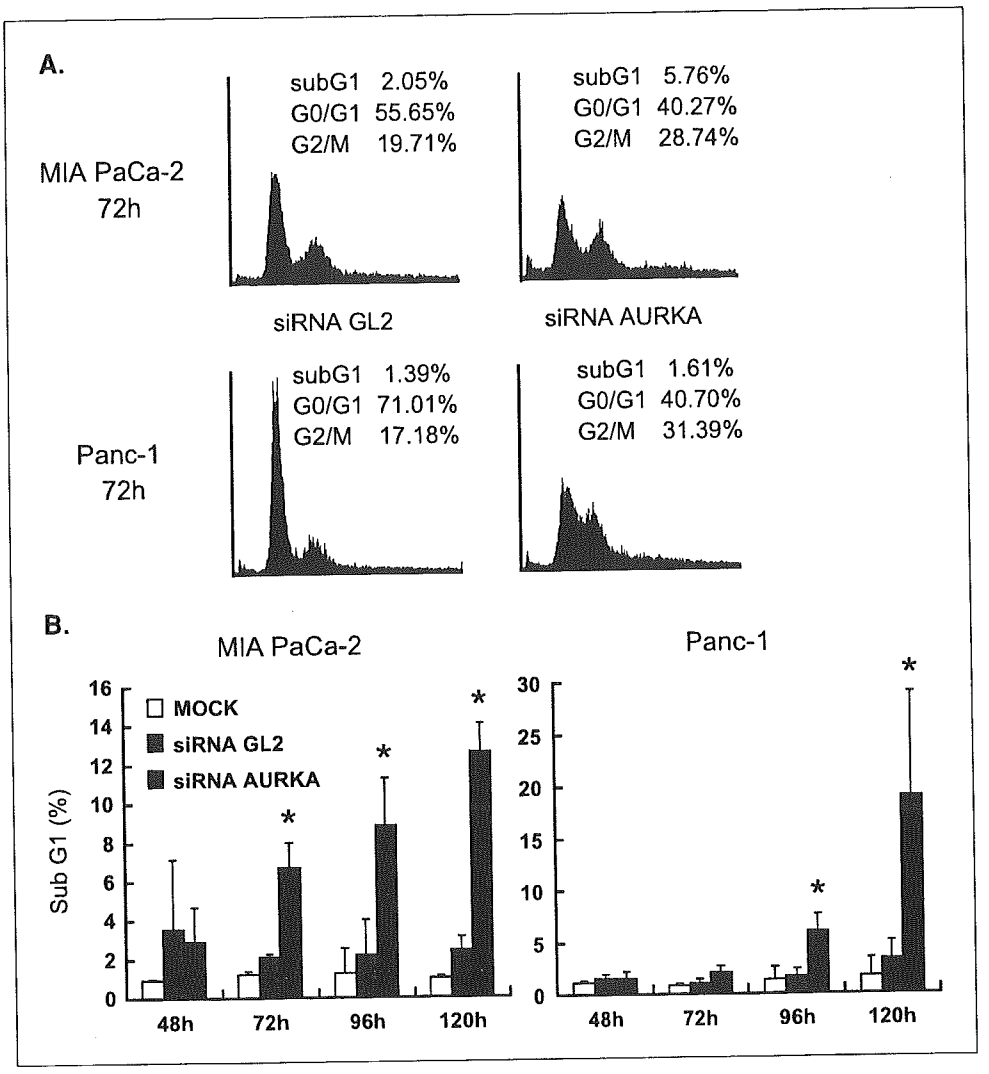

Figure 4. siRNA directed against *AURKA* induces G2/M accumulation and eventual apoptosis. *A*, cells were collected 72 hours after siRNA transfection at 200 nmol/L and subsequently assayed for their DNA content by flow cytometry. These experiments were performed for four times. Representative results are shown. *B*, time course quantification of sub-G1 population after siRNA transfection at 200 nmol/L. These experiments were performed for four times. *, $P < 0.05$.

tested the potential enhancement of the cytotoxic effect of taxanes by *AURKA*-siRNA by treating cells either with *AURKA* or *GL2*-siRNA at 10 nmol/L in concentration followed by addition of either 10 nmol/L paclitaxel or 5 nmol/L docetaxel 4 hours later. After 72 hours of incubation, the viabilities of the cells were measured by MTT assay. Although the modest *AURKA*-siRNA at 10 nmol/L alone did not show any difference in cytotoxic effect when compared with the control treatment with*GL2*-siRNA, it enhanced the cytotoxic effects induced by taxanes significantly more strongly than the control treatment (Fig. 5*A*). A reciprocal set of experiments showed that taxanes can enhance the cytotoxic effect of *AURKA*-siRNA, as shown in Fig. 5*B*; the synergistic enhancement of the cytotoxic effect of *AURKA*-siRNA by taxanes were obvious from the treatment at 10 nmol/L siRNA and accelerated with increasing doses. These results indicate that the RNAi-mediated knockdown of AURKA can synergistically enhance the chemosensitivities of these pancreatic cancer cells to taxanes.

Discussion

AURKA is a commonly amplified and overexpressed gene in various types of cancers, including pancreatic cancer. In attempting to determine the possibility of AURKA as a therapeutic target, we employed the RNAi technique for knockdown of its expression and analyzed its phenotype. We found that a transient knockdown of AURKA strikingly inhibited growth and colony formation of pancreatic cancer cells *in vitro*. Stable suppression of AURKA in pancreatic cancer cells revealed an almost complete abrogation of their tumorigenicity in a mouse xenograft model. The knockdown induced accumulation of the cells in the G_2-M phase and eventual apoptosis. Rojanala et al. (23) recently reported that antisense oligonucleotide mediated transient suppression of AURKA resulted in growth suppression, G_2-M arrest, and eventual apoptosis *in vitro*. Our results are in good agreement with theirs. We further showed that the knockdown of *AURKA* significantly enhanced the cytotoxic effect of taxanes. Our findings indicate that AURKA is an attractive candidate for a therapeutic target, because it can regress tumorigenicity and enhance chemosensitivity to taxanes in pancreatic cancer.

We were able to achieve almost complete suppression of *AURKA* expression by using our siRNA treatment strategy in pancreatic cancer cells. The knockdown of AURKA induced the strong suppression of growth, accumulation in G_2-M phase, and eventual apoptosis of the cells. This result suggests that AURKA is an

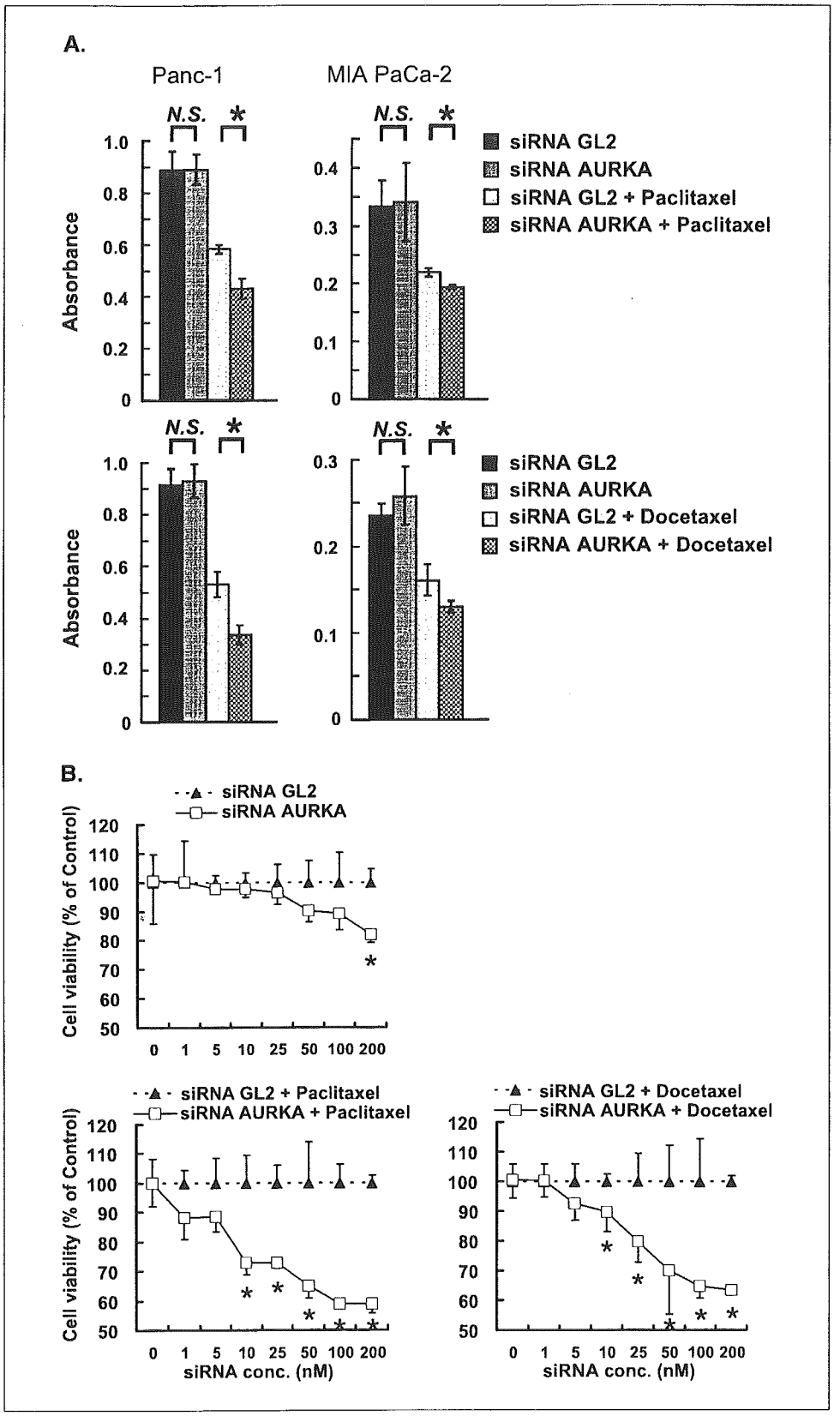

Figure 5. Synergistic enhancement of cytotoxicity between siRNA directed against *AURKA* and taxanes. *A*, survival cells quantitated by MTT assay after siRNA transfection targeting *AURKA* or *luciferase* (GL2) at 10 nmol/L only or subsequent addition of 10 nmol/L paclitaxel or 5 nmol/L docetaxel. These experiments were performed for four times. *, $P < 0.05$. *N.S.*, not significantly different. *B*, survival cells quantitated by MTT assay after various doses of siRNA transfection targeting *AURKA* or *luciferase* (*GL2*) only or subsequent addition of 10 nmol/L paclitaxel or 5 nmol/L docetaxel. Values were normalized by dividing them by control values of siRNA-GL2 at each concentration. These experiments were performed for four times. *, $P < 0.05$.

essential molecule for proliferation of cancer cells and a good target for halting proliferation and triggering apoptosis; this can be explained by its key roles in mitosis, as we expected. More strikingly, the knockdown of *AURKA* completely inhibited tumorigenesis *in vivo*, even in the modest suppression of its expression achieved by our stable vector-mediated shRNAi strategy. This result suggests that overexpression of AURKA is strongly associated with the *in vivo* tumorigenic ability of pancreatic cancer cells,

leading us to an interpretation of the frequent overexpression of *AURKA* in primary pancreatic cancer tissues and to an expectation that the knockdown strategy will be practical in stopping the progression of the cancer *in vivo*.

We found that the RNAi-mediated knockdown of *AURKA* synergistically enhanced the cytotoxicity of taxanes. Taxanes bind to free tubulin and promote the assembly of tubulin into stable microtubules by interfering with their disassembly. They inhibit cell cycle progression by accumulating cells in M phase at the metaphase-anaphase transition and subsequently lead them to apoptosis. Knockdown of *AURKA* also induced accumulation of cells in the G_2-M phase and led to eventual apoptosis. As we noted, AURKA is essential for the proper arrangement of centrosomes and microtubules. Our results suggest that the combination of *AURKA* knockdown and taxanes results in strong impairment of M phase progression and the synergistic induction of apoptosis. This is consistent with the recent report indicating that HeLa cells with overexpression of *AURKA* gained a resistance to paclitaxel by decreasing spindle checkpoint activity (24). In that report, Anand et al. noted that overexpression of AURKA may decrease spindle checkpoint activity. In our experiments, *AURKA* knockdown may have recovered spindle checkpoint activity and thus increased the sensitivity of taxanes. The mechanism that triggers apoptosis by AURKA knockdown remains to be clarified. Taxanes have cytotoxic activity against various types of cancers including pancreatic cancer. Docetaxel is used for pancreatic cancers as first-line chemotherapy or a second-line combination with gemcitabine in phase II clinical trials (25, 26). Paclitaxel has been used as a radiation sensitizer (27). These taxane-mediated chemotherapies could be more effective in combination with knockdown of *AURKA*.

RNAi is becoming a conventional application for *in vivo* cancer therapy (28, 29). An efficient delivery system of siRNA into solid tumors has been developed (30). Our results suggest that RNAi-mediated knockdown of AURKA can be used as a specific gene-targeting therapy to suppress progression of pancreatic cancer. Interestingly, in a recent report, Harrington et al. developed a selective small-molecule inhibitor of Aurora kinases, VX-680, and showed a potent antitumor activity (31). We can assume that this different type of approach is also promising for *in vivo* abrogation of progression in pancreatic cancer.

Acknowledgments

Received 11/5/2004; revised 1/5/2005; accepted 1/25/2005.

Grant support: Ministry of Education, Culture, Science, Sports, and Technology of Japan.

The costs of publication of this article were defrayed in part by the payment of page charges. This article must therefore be hereby marked *advertisement* in accordance with 18 U.S.C. Section 1734 solely to indicate this fact.

We thank Dr. Barbara Lee Smith Pierce (a professor with the University of Maryland University College) for editorial work in the preparation of this article.

References

1. Bardeesy N, DePinho RA. Pancreatic cancer biology and genetics. Nat Rev Cancer 2002;2:897–909.
2. Pietras RJ, Pegram MD, Finn RS, Maneval DA, Slamon DJ. Remission of human breast cancer xenografts on therapy with humanized monoclonal antibody to HER-2 receptor and DNA-reactive drugs. Oncogene 1998;17:2235–49.
3. Ranson M, Hammond LA, Kris M, et al. ZD1839, a selective oral epidermal growth factor receptor-tyrosine kinase inhibitor, is well tolerated and active in patients with solid, malignant tumors: results of a phase I trial. J Clin Oncol 2002;20:2240–50.
4. Jaffee EM, Hruban RH, Canto M, Kern SE. Focus on pancreas cancer. Cancer Cell 2002;2:25–8.
5. Furukawa T, Horii A. Molecular pathology of pancreatic cancer: in quest of tumor suppressor genes. Pancreas 2004;28:253–6.
6. Fukushige S, Waldman FM, Kimura M, et al. Frequent gain of copy number on the long arm of chromosome 20 in human pancreatic adenocarcinoma. Genes Chromosomes Cancer 1997;19:161–9.
7. Aguirre AJ, Brennan C, Bailey G, et al. High-resolution characterization of the pancreatic adenocarcinoma genome. Proc Natl Acad Sci U S A 2004; 101:9067–72.
8. Bischoff JR, Anderson L, Zhu Y, et al. A homologue of *Drosophila* aurora kinase is oncogenic and amplified in human colorectal cancers. EMBO J 1998; 17:3052–65.
9. Tanaka T, Kimura M, Matsunaga K, Fukada D, Mori H, Okano Y. Centrosomal kinase AIK1 is overexpressed in invasive ductal carcinoma of the breast. Cancer Res 1999;59:2041–4.
10. Sen S, Zhou H, Zhang RD, et al. Amplification/overexpression of a mitotic kinase gene in human bladder cancer. J Natl Cancer Inst 2002;94:1320–9.
11. Gritsko TM, Coppola D, Paciga JE, et al. Activation and overexpression of centrosome kinase BTAK/Aurora-A in human ovarian cancer. Clin Cancer Res 2003;9:1420–6.
12. Jeng YM, Peng SY, Lin CY, Hsu HC. Overexpression and amplification of Aurora-A in hepatocellular carcinoma. Clin Cancer Res 2004;10:2065–71.
13. Sen S, Zhou H, White RA. A putative serine/threonine kinase encoding gene BTAK on chromosome 20q13 is amplified and overexpressed in human breast cancer cell lines. Oncogene 1997;14:2195–200.
14. Crane R, Gadea B, Littlepage L, Wu H, Ruderman JV. Aurora A, meiosis and mitosis. Biol Cell 2004;96:215–29.
15. Zhou H, Kuang J, Zhong L, et al. Tumour amplified kinase STK15/BTAK induces centrosome amplification, aneuploidy and transformation. Nat Genet 1998;20: 189–93.
16. Elbashir SM, Harborth J, Lendeckel W, Yalcin A, Weber K, Tuschl T. Duplexes of 21-nucleotide RNAs mediate RNA interference in cultured mammalian cells. Nature 2001;411:494–8.
17. Kobari M, Hisano H, Matsuno S, Sato T, Kan M, Tachibana T. Establishment of six human pancreatic cancer cell lines and their sensitivities to anti-tumor drugs. Tohoku J Exp Med 1986;150:231–48.
18. Kufer TA, Sillje HH, Korner R, Gruss OJ, Meraldi P, Nigg EA. Human TPX2 is required for targeting Aurora-A kinase to the spindle. J Cell Biol 2002;158:617–23.
19. Hirota T, Kunitoku N, Sasayama T, et al. Aurora-A and an interacting activator, the LIM protein Ajuba, are required for mitotic commitment in human cells. Cell 2003;114:585–98.
20. Kondo E, Horii A, Fukushige S. The human PMS2L proteins do not interact with hMLH1, a major DNA mismatch repair protein. J Biochem 1999;125:818–25.
21. Brummelkamp TR, Bernards R, Agami R. A system for stable expression of short interfering RNAs in mammalian cells. Science 2002;296:550–3.
22. Marumoto T, Honda S, Hara T, et al. Aurora-A kinase maintains the fidelity of early and late mitotic events in HeLa cells. J Biol Chem 2003;278:51786–95.
23. Rojanala S, Han H, Muñoz RM, et al. The mitotic serine threonine kinase, Aurora-2, is a potential target for drug development in human pancreatic cancer. Mol Cancer Ther 2004;3:451–7.
24. Anand S, Penrhyn-Lowe S, Venkitaraman AR. AURORA-A amplification overrides the mitotic spindle assembly checkpoint, inducing resistance to taxol. Cancer Cell 2003;3:51–62.
25. Lenzi R, Yalcin S, Evans DB, Abbruzzese JL. Phase II study of docetaxel in patients with pancreatic cancer previously untreated with cytotoxic chemotherapy. Cancer Invest 2002;20:464–72.
26. Ryan DP, Kulke MH, Fuchs CS, et al. A phase II study of gemcitabine and docetaxel in patients with metastatic pancreatic carcinoma. Cancer 2002; 94:97–103.
27. Safran H, Moore T, Iannitti D, et al. Paclitaxel and concurrent radiation for locally advanced pancreatic cancer. Int J Radiat Oncol Biol Phys 2001; 49:1275–9.
28. Brummelkamp TR, Bernards R, Agami R. Stable suppression of tumorigenicity by virus-mediated RNA interference. Cancer Cell 2002;2:243–7.
29. Hingorani SR, Jacobetz MA, Robertson GP, Herlyn M, Tuveson DA. Suppression of BRAF(V599E) in human melanoma abrogates transformation. Cancer Res 2003; 63:5198–202.
30. Takei Y, Kadomatsu K, Yuzawa Y, Matsuo S, Muramatsu T. A small interfering RNA targeting vascular endothelial growth factor as cancer therapeutics. Cancer Res 2004;64:3365–70.
31. Harrington EA, Bebbington D, Moore J, et al. VX-680, a potent and selective small-molecule inhibitor of the Aurora kinases, suppresses tumor growth *in vivo*. Nat Med 2004;10:262–7.

Intrinsic Chemoresistance to Gemcitabine Is Associated with Decreased Expression of BNIP3 in Pancreatic Cancer

Masanori Akada,[1,2] Tatjana Crnogorac-Jurcevic,[1] Samuel Lattimore,[1] Patrick Mahon,[1] Rita Lopes,[1] Makoto Sunamura,[1,2] Seiki Matsuno,[2] and Nicholas R. Lemoine[1]

Abstract **Purpose:** Although chemotherapy with gemcitabine is a common mode of treatment of pancreatic cancer, 75% of patients do not benefit from this therapy. It is likely that the sensitivity of cancer cells to gemcitabine is determined by a number of different factors.

Experimental Design: To identify genes that might contribute to resistance to gemcitabine, 15 pancreatic cancer cell lines were subjected to gemcitabine treatment. Simultaneously, gene expression profiling using a cDNA microarray to identify genes responsible for gemcitabine sensitivity was performed.

Results: The pancreatic cancer cell lines could be classified into three groups: a gemcitabine "sensitive," an "intermediate sensitive," and a "resistant" group. Microarray analysis identified 71 genes that show differential expression between gemcitabine-sensitive and -resistant cell lines including 27 genes relatively overexpressed in sensitive cell lines whereas 44 genes are relatively overexpressed in resistant cell lines. Among these genes, 7 genes are potentially involved in the phosphatidylinositol 3-kinase/Akt pathway. In addition to this major signaling pathway, Bcl2/adenovirus E1B 19 kDa protein interacting protein (BNIP3), a Bcl-2 family proapoptotic protein, was identified as being expressed at lower levels in drug-resistant pancreatic cancer cell lines. In an analysis of 21 pancreatic cancer tissue specimens, more than 90% showed down-regulated expression of BNIP3. When expression of BNIP3 was suppressed using small interfering RNA, gemcitabine-induced cytotoxicity *in vitro* was much reduced.

Conclusions: These results suggest that BNIP3 and the phosphatidylinositol 3-kinase/Akt pathway may play an important role in the poor response to gemcitabine treatment in pancreatic cancer patients.

Pancreatic adenocarcinoma is a common cancer with an extremely poor prognosis. It is the fourth leading cause of cancer death in the United States (1). Despite an enormous amount of effort spent in the development of cancer chemotherapies for pancreatic cancer, these are effective only in a small proportion of patients. Along with a lack of early diagnostic tests that might allow surgical intervention at a potentially curable stage, this is one of the major problems in the management of pancreatic cancer.

In the past few years, gemcitabine [2′,2′-difluorodeoxycitidine, Gemzar, Eli-Lilly, Indianapolis, IN), a novel pyrimidine nucleoside analogue, has become the standard chemotherapeutic agent used in patients with pancreatic cancer. A phase II randomized trial in advanced pancreatic cancer showed that gemcitabine was more effective than 5-fluorouracil (2, 3).

However, not more than 25% of patients with pancreatic cancer will benefit from gemcitabine, a proportion that is slightly less than in patients with other cancers (4). It has long been recognized that the effectiveness of anticancer drugs can vary significantly between individual patients. Several attempts have already been undertaken in both cell lines and clinical samples to detect molecular markers of gemcitabine chemosensitivity. Such markers can be categorized into two groups. The majority of genes are related to nucleoside transport and metabolism, which may be involved in the intracellular handling of gemcitabine in cancer cells. In this category, nucleoside transporter (5, 6), M1 or M2 subunit of ribonucleoside reductase (7–11), and deoxycytidine kinase (12) have all been described as being related to gemcitabine chemosensitivity. Another group comprises the genes involved in cell cycle regulation, proliferation, or apoptosis. Mutated p53 (13) and Bcl-xl (14, 15) have been identified as possible molecular markers for gemcitabine chemoresistance, and both are directly involved in apoptosis. In addition, c-Src (16, 17) and focal adhesion kinase (FAK; ref. 18) were also described as gemcitabine resistance–related genes. These genes may be involved in resistance of pancreatic cells to gemcitabine by activating the phosphatidylinositol 3-kinase (PI3K)/Akt pathway. Furthermore, another study

Authors' Affiliations: [1]Cancer Research UK Clinical Centre at Barts and London School of Medicine, London, United Kingdom and [2]Division of Gastroenterological Surgery, Department of Surgery, Tohoku University School of Medicine, Sendai, Japan

Received 9/2/04; revised 12/14/04; accepted 1/5/05.

The costs of publication of this article were defrayed in part by the payment of page charges. This article must therefore be hereby marked *advertisement* in accordance with 18 U.S.C. Section 1734 solely to indicate this fact.

Requests for reprints: Nicholas R. Lemoine, Molecular Oncology Unit, Cancer Research UK Clinical Centre at Barts and London School of Medicine, John Vane Science Building, Charterhouse Square, London EC1M 6BQ, United Kingdom. Phone: 44-20-7014-0420; Fax: 44-20-7014-0431; E-mail: nick.lemoine@cancer.org.uk.

showed that under hypoxic conditions pancreatic cancer cell lines become resistant to apoptosis primarily by activation of PI3K/Akt and nuclear factor κB pathways, as well as partially through the mitogen-activated protein (MAP) kinase signaling pathway (19).

It is clear that the sensitivity/resistance of cancer cells to gemcitabine cannot be predicted by a single factor but may be determined by the balance of many factors. Therefore, to establish the baseline for prediction of chemosensitivity, a comprehensive analysis of the sets of genes that characterize the response of cancer cells to gemcitabine treatment is needed.

During the past few years, cDNA/oligonucleotide microarray analysis has become a key tool for characterizing gene expression in a variety of experimental systems, and it has also been used for detecting gemcitabine chemosensitivity markers. So far, two studies have been reported (9, 10). In both of them, cell clones that had acquired resistance *in vitro* were compared with their chemosensitive parental cell lines. However, it is important to use nontreated cell lines to identify genetic factors that determine intrinsic (as opposed to acquired) chemoresistance, as this more closely represents the clinical situation at presentation of a cancer patient. In this study, by analyzing 15 different pancreatic cancer cell lines with a range of gemcitabine sensitivity, we attempted to identify novel genes associated with intrinsic gemcitabine resistance using a cDNA microarray system consisting of 9,464 human gene elements.

Materials and Methods

Pancreatic cancer tissues and cell lines. Sixteen human pancreatic cancer cell lines were used in this study: A818.4, AsPc-1, CFPAC-1, FA6, Hs766T, MDAPanc-3, MiaPaCa-2, PANC-1, PaTu-I, RWP-1, Suit-2, and T3M4 were obtained from Cancer Research UK cell production services. PK1, PK9, and PK59 were established and maintained at Tohoku University (20). All cell lines were kept in a humidified incubator at 37°C with 5% CO_2 and cultured in E4 complete medium, supplemented with 10% fetal bovine serum, penicillin (0.1 μg/mL), and streptomycin (100 units/mL). The human pancreatic ductal epithelial cell line HPDE was a kind gift from Dr. Ming-Sound Tsao (University of Toronto, Canada) and was grown in keratinocyte medium as described before (21).

Pancreatic cancer tissues were obtained from the Human Biomaterials Resource Centre (Hammersmith Hospital, London, United Kingdom) and Tohoku University Hospital (Sendai, Japan) with full ethical approval from the host institutions. All tissues used were enriched for the tumor cellular component (60-80%) by trimming freshly frozen blocks whereas performing H&E sections at frequent levels as described previously (22).

Total RNA extraction from cell lines and tissues was done using Trizol reagent (Invitrogen, Renfrew, Renfrewshire, United Kingdom) according to the protocol of the manufacturer.

3-(4,5-Dimethylthiazol-2-yl)-2,5-diphenyltetrazolium bromide assay. Cells were resuspended in fresh medium at a concentration of 1×10^4 cells/well and seeded in a 96-well plate. Cells were incubated for 24 hours at 37°C, and then gemcitabine at various concentrations was added to each well. The plate was incubated at 37°C for a further 72 hours. For the assay, 10 μL of 3-(4,5-dimethylthiazol-2-yl)-2,5-diphenyltetrazolium bromide (5 mg/mL) were added to each well and the plate was incubated for an additional 3 hours at room temperature. The absorbance was measured at 560 nm using a microplate reader (Dynex, Worthing, United Kingdom).

Microarray hybridization. The 10K cDNA Sanger Human Arrays (version 1.2.1) obtained through the Cancer Research-UK/Ludwig Institute/Wellcome Trust consortium were used in this study. They contain 9,464 human gene elements. The glass arrays were manufactured and quality controlled at the Sanger Centre (Cambridge, United Kingdom). The spotting pattern and the complete annotated list of these cDNAs are available at the CRUK Microarray web site (http://www.sanger.ac.uk/Projects/Microarrays/informatics/hver1.2.1.shtml).

Labeling of 50 μg of total RNA was achieved by direct incorporation of Cy5-dCTP or Cy3-dCTP (Amersham Pharmacia Biotech, Amersham, United Kingdom) in a reverse transcription reaction using anchored oligodeoxythymidylate primers (Cancer Research-UK Oligonucleotide Service, London Research Institute, Clare Hall Laboratories, United Kingdom) and Superscript II reverse transcriptase (Invitrogen). The details of the hybridization and washing protocols are available online (http://www.cgal.icnet.uk/exprotocols/protocols.html).

The cDNA derived from the HPDE cell line was used as the control sample in all hybridizations. In each experiment, Cy5-dCTP–tagged cDNA from an individual pancreatic cancer cell line was mixed with Cy3-dCTP–tagged cDNA from HPDE cells and subsequently cohybridized to a microarray. All the experiments were done in duplicate.

Following hybridization, arrays were scanned using an Affymetrix 428 dual-laser microarray (Affymetrix, Santa Clara, CA) and separate images were acquired for Cy3 and Cy5 fluorescence.

Image and data analysis. The signal intensity values of each element were extracted using the ImaGene 5 software program (BioDiscovery, Los Angeles, CA). Normalization of the resulting spot intensities was achieved through the VSN package as part of the Bioconductor software within R (23). Differentially expressed genes were isolated by permutation testing using the t statistic (perm = 10,000) and subsequent P value correction using the false discovery rate method of Benjamini et al. (24). Differentially expressed genes were those that had a corrected P value of <0.05. Sample-wise agglomerative hierarchical clustering was carried out by first selecting the top 1,000 genes based on variance, then using Euclidean distance to generate the distance matrix, and average linkage to group the samples. All of these were done within the R environment.

Quantitative real-time reverse transcription-PCR. Primers were designed using the Primer Express software (Applied Biosystems, Foster City, CA). The primer sequences for Bcl2/adenovirus E1B 19 kDa protein interacting protein (BNIP3; 61 bp amplicon) are as follows: forward, 5′-GTGGTCAAGTCGGCCGG-3′; reverse; 5′-GCGC-TTCGGGTGTTTAAAGA-3′.

Template cDNAs were synthesized from 1.5 μg of total RNA using the Taqman reverse transcription reaction kit (Applied Biosystems).

The real-time reverse transcription-PCR (RT-PCR) reactions were set up in a total volume of 20 μL using 3 μL of cDNA and 10 μL of SYBR Green Master Mix (Applied Biosystems). The final primer concentration was 300 mmol/L for both forward and reverse primers. For every target gene a set of triplicate reactions using five dilutions of reverse-transcribed Universal Human reference RNA (Stratagene, LA Jolla, CA) was included to construct a standard curve. No-template control reactions were also included. Real-time RT-PCR was done using the ABI 7700 sequence detector (Applied Biosystems).

RNA interference. Custom-made oligonucleotide small interfering RNA (siRNA; SMARTpool) for BNIP3 was obtained from Dharmacon (Lafayette, CO), lamin siRNA was obtained from Qiagen GmbH (Hilden, Germany), and nonsilencing negative control siRNA was obtained from Ambion (Austin, TX). The 2×10^5 cells were seeded into a six-well plate and allowed to adhere for 24 hours. Aliquots of 150 pmol of siRNA, 4 μL of Enhancer R (Qiagen), and 93 μL of Buffer EC-R (Qiagen) were mixed and vortexed. After 5 minutes of incubation at room temperature, 8 μL of TransMessenger transfection reagent (Qiagen) were mixed together, then incubated for 10 minutes at room temperature. This siRNA/agent mixture was added into the wells with 800 μL of serum-free/antibiotic-free E4 medium and incubated for 3 hours, after which the medium was changed to 1 mL DMEM with 10%

fetal bovine serum. Twenty-four hours posttransfection, cells were trypsinized, seeded into a 96-well plate, and used for the cell growth inhibition assay.

Western blot analysis. The 2×10^6 cells were harvested and rinsed twice with PBS, at pH 7.4. Cell extracts were prepared with lysis buffer [20 mmol/L Tris (pH 7.5), 0.1% Triton X-100, 0.5% deoxycholate, 1 mmol/L phenylmethylsulfonyl fluoride, 10 μg/mL aprotinin, and 10 μg/mL leupeptin]. Total protein concentration was measured using the Protein assay kit with bovine serum albumin as a standard, according to the instructions of the manufacturer (Bio-Rad, Hercules, CA). Cell extracts containing 40 μg of total protein were subjected to electrophoresis in 10% SDS/PAGE gels and after transfer and blocking with PBS containing 0.2% bovine serum albumin for 16 hours at 4°C, the membrane was incubated with 2 μg/mL mouse monoclonal anti-BNIP3 antibody clone Ana 40 (Sigma-Aldrich, St. Louis, MO). The incubation was for 2 hours at room temperature, followed by washing with 0.1% Tween 20/PBS thrice, and then incubation with secondary antibody mouse immunoglobulin G (Santa Cruz Biotechnology, Santa Cruz, CA) for 30 minutes followed by three washes.

Signals were detected by chemiluminescence using the enhanced chemiluminescence detection system (Amersham Biosciences).

Results

Efficacy of cytotoxicity induced in pancreatic cancer cell lines by gemcitabine exposure. The responses of 15 pancreatic cancer cell lines to gemcitabine treatment were investigated using the 3-(4,5-dimethylthiazol-2-yl)-2,5-diphenyltetrazolium bromide assay. Representative dose-response curves are shown in Fig. 1A and B. Three cell lines (CFPAC-1, Suit-2, and T3M4) showed high sensitivity to gemcitabine with less than 20% of those cells surviving in the presence of 25 ng/mL of gemcitabine for 72 hours (Fig. 1A) and their IC_{50} values were 0.5, 0.7, and 3.0 ng/mL, respectively. Hence, these three cell lines were classified as the "sensitive" group. In contrast, three cell lines (Hs766T, RWP-1, and A818.4) showed low sensitivity, with more than 60% of those cells surviving even in the presence of more than 1×10^4 ng/mL of the drug for 72 hours (Fig. 1B). These three cell lines were therefore classified as "resistant." The remaining cell lines (AsPc-1, FA6, MDAPanc-3, MiaPaCa-2, PANC-1 PaTu-I, PK1, PK9, and PK59) showed moderate sensitivity (IC_{50} values 5-1,000 ng/mL) and were classified as "intermediate sensitive." Figure 1C shows the dose-response curve for the immortalized pancreatic ductal cell line HPDE (IC_{50} 0.8 ng/mL).

Genes involved in gemcitabine chemosensitivity. To identify genes differentially expressed between sensitive and resistant cell lines, cDNA microarray experiments were carried out using mRNA extracted from all cell lines. In a comparison between the sensitive and resistant groups, 71 genes were identified that show differential expression between the two groups (Tables 1 and 2).

Of these 71 genes, 27 genes are relatively overexpressed in gemcitabine-sensitive cell lines, and 44 are relatively overexpressed in gemcitabine-resistant cell lines. Genes with a wide variety of functions were identified among these genes, with a large proportion that could be categorized into two groups: 14 genes are related to gemcitabine metabolism and transport (genes 1-8 in Table 1 and genes 28-33 in Table 2) and 27 genes are related to signaling pathways for cell cycle regulation, proliferation, or apoptosis (genes 9-16 in Table 1 and genes 34-52 in Table 2). Among these, FAK was already described as a gemcitabine sensitivity–related gene (18). In contrast, although nucleoside transporter 1 (5, 6), ribonucleoside reductase M1 and M2 (7–11), and deoxycytidine kinase (12) were previously described as gemcitabine sensitivity–related genes, they showed no significant difference between gemcitabine-sensitive cell lines and gemcitabine-resistant cell lines in our experiments. Other genes in this class that were previously described as gemcitabine sensitivity related were not included in our microarray. Also, seven genes are potentially involved in the PI3K/Akt pathway: *PXN*, *p70S6K*, *FAK*, *PIK3C3*, *TSC1*, *IGFBP7*, and *ITGA9*. A further three genes are related to the transforming growth factor-β (TGF-β) signaling pathway: *RALBP1*, *SMAD2*, and *LTBP1*.

Interestingly, among the selected genes, several are located at the same chromosomal regions such as 6q (MAP3K7, *C6orf93*, and *HECA*), 10q (*BNIP3*, *PPP3CB*, *KIAA0261*, and *MGEA5*), 19q (*EBP*, *PPP1R15A*, and *LRP3*), and 22q (*CDC42EP*, *FLJ22582*, *SLC25A1*, and *TCN2*), and these loci are also previously reported as sites of frequent aberrations and amplification in pancreatic cancer (25–27). In addition,

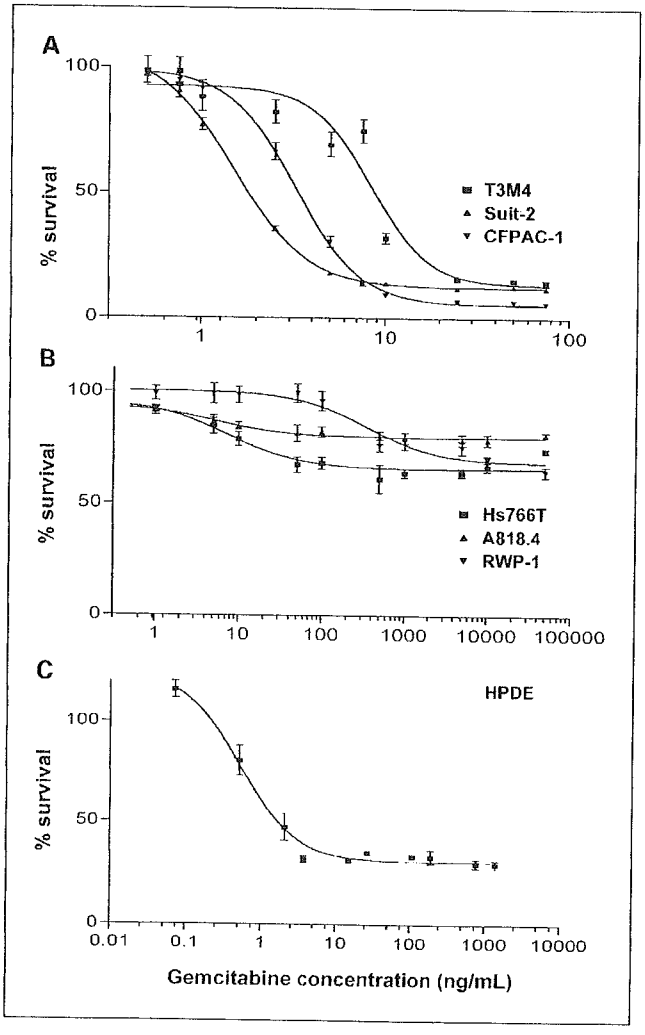

Fig. 1. Dose-response curves for gemcitabine in pancreatic cancer cell lines. *A*, gemcitabine-sensitive cell lines: CFPAC-1, Suit-2, and T3M4. *B*, gemcitabine-resistant cell lines: RWP-1, A818.4, and Hs766T. *C*, HPDE. Points, mean; bars, SD.

Table 1. Genes relatively overexpressed in gemcitabine-sensitive pancreatic cancer cell lines

No.	Common name	Unigene ID	Description	Chromosomal location	*P*	*t*
Genes involved in nucleoside metabolism and transportation						
1	*PAICS*	Hs.444439	phosphoribosylaminoimidazole carboxylase	4q12	1.65e-06	−9.9914
2	*CDC42EP1*	Hs.148101	CDC42 effector protein (Rho GTPase binding) 1	22q13.1	5.95e-05	−6.65
3	*TNNI3*	Hs.512709	troponin I, cardiac	19q13.42	0.00071	−5.8469
4	*DNM1*	Hs.436132	dynamin 1	9q34.11	0.0002	−5.778
5	*EBP*	Hs.196669	emopamil binding protein (sterol isomerase)	Xp11.23	0.0006	−5.6273
6	*SMARCA3*	Hs.3068	SWI/SNF related, matrix associated, actin dependent regulator of chromatin, subfamily a, member 3	3q24	0.00058	−5.4641
7	*P2RX4*	Hs.321709	purinergic receptor P2X, ligand-gated ion channel, 4	12q24.31	0.00042	−5.3659
8	*CDA*	Hs.72924	cytidine deaminase	1p36.12	0.00092	−4.822
Genes involved in signaling pathways for cell cycle regulation, proliferation, or apoptosis.						
9	*IGFBP7*	Hs.435795	insulin-like growth factor binding protein 7	4q12	4.00e-08	−17.251
10	*p70S6K*	Hs.86858	Ribosomal protein S6 kinase, 70kDa	17q11.2	0.00012	−8.0003
11	*BNIP3*	Hs.79428	Bcl2/adenovirus E1B 19 kDa protein interacting protein	10q26.3	0.00014	−7.5318
12	*PXN*	Hs.446336	paxillin	12q24.23	0.00017	−6.2075
13	*CHAF1B*	Hs.75238	chromatin assembly factor 1, subunit B (p60)	21q22.13	0.00039	−5.3061
14	*RBMS2*	Hs.438778	RNA binding motif, single stranded interacting protein 2	12q23.2	0.00045	−5.267
15	*RGS2*	Hs.78944	regulator of G-protein signaling 2, 24 kDa	1q31.2	0.00048	−5.0793
16	*CREM*	Hs.231975	cyclic AMP responsive element modulator	10p11.21	0.00059	−4.9462
Unknown and other function						
17	*PCCB*	Hs.63788	propionyl CoA carboxylase, β polypeptide	3q22.1	1.83e-05	−8.037
18	*MPDZ*	Hs.169378	multiple PDZ domain protein	9p23	0.00012	−7.0767
19	*SGCE*	Hs.409798	sarcoglycan, epsilon	7q21.3	0.00048	−7.0147
20	*GPSN2*	Hs.306122	glycoprotein, synaptic 2	4q22.1	9.46e-05	−6.6151
21	*LMNB1*	Hs.89497	lamin B1	5q23.1	7.21e-05	−6.4772
22	*FLJ22582*	Hs.126783	hypothetical protein FLJ22582	22q13.1	0.00019	−5.7262
23	*DHCR7*	Hs.11806	7-dehydrocholesterol reductase	11q13.1	0.00039	−5.4782
24	*SERPINF2*	Hs.159509	serine proteinase inhibitor, clade F, member 2	17p13.3	0.00079	−5.3929
25	*SLC25A1*	Hs.111024	solute carrier family 25 , member 1	22q11	0.00069	−5.0347
26	*TCN2*	Hs.417948	transcobalamin II; macrocytic anemia	22q12.2	0.00071	−5.0308
27	*RDX*	Hs.263671	radixin	11q22.3	0.00092	−4.6462

several other genes were also located at frequently aberrant sites such as 3p, 3q, 5p, 8p, 8q, 9p, 17p, 17q, 18p, 19p, and 20q.

Expression profiling and clustering. To investigate whether cell lines grouped as either sensitive or resistant are also genetically similar, hierarchical clustering was done as described in Materials and Methods, and this was able clearly to separate gemcitabine-resistant and gemcitabine-sensitive cell lines.

It is also evident that all the replicates for analyses of individual cell lines are situated close to each other, indicating the overall reproducibility of the array technique (Fig. 2).

BNIP3 down-regulation is associated with chemoresistance of pancreatic cancer to gemcitabine. We have selected BNIP3 as a candidate gene involved in chemosensitivity for further analysis. The expression of BNIP3 mRNA was examined in all pancreatic cell lines by quantitative real-time RT-PCR, and the data obtained were in a complete agreement with our cDNA microarray results. It is evident that in comparison with HPDE, BNIP3 expression was down-regulated in all pancreatic cancer cell lines analyzed except PANC-1 and CFPAC-1. Especially in resistant but also in intermediate sensitive cell lines, BNIP3 expression levels were down-regulated more than 90% (Fig. 3A). Only the PANC-1 cell line in the intermediate sensitive group showed an expression level comparable to that of the immortalized normal cell line HPDE.

BNIP3 expression is down-regulated in pancreatic cancer. To explore if the expression level of BNIP3 in clinical specimens corresponds to the data obtained in cell lines, quantitative real-time RT-PCR analysis was done using mRNA extracted from tissues from 21 different patients with pancreatic adenocarcinoma. Figure 3B shows the expression compared with a control pancreatic tissue from a healthy donor. In all but two (T1 and T20) of the cancer specimens, BNIP3 expression levels were reduced compared with the normal control, and in 14 of 21 samples more than 50% down-regulation of BNIP3 expression was observed.

BNIP3 siRNA treatment increases chemoresistance of pancreatic cancer cells to gemcitabine. To verify that BNIP3 is involved in gemcitabine sensitivity, siRNA experiments were

Table 2. Genes relatively overexpressed in gemcitabine-resistant pancreatic cancer cell lines

No.	Common name	Unigene ID	Description	Chromosomal location	*P*	*t*
Genes for nucleoside metabolism and transportation						
28	*DYT1*	Hs.278429	*Homo sapiens* dystonia 1, torsion	9q34.11	5.76e-05	7.10491
29	*VIPR1*	Hs.348500	vasoactive intestinal peptide receptor 1	3p22.1	0.00014	6.50633
30	*ATP11C*	Hs.88252	ATPase, Class VI, type 11C	Xq27.1	0.00055	5.55326
31	*MTSS1*	Hs.77694	metastasis suppressor 1	8q24.13	0.00051	5.52812
32	*SAFB*	Hs.23978	scaffold attachment factor B	19p13.2	0.00068	5.13198
33	*RALBP1*	Hs.75447	ralA binding protein 1	18p11.22	0.00075	4.7879
Genes involved in signaling pathways for cell cycle regulation, proliferation, or apoptosis.						
34	*SMAD2*	Hs.110741	SMAD, mothers against DPP homologue 2	18q21.1	4.3e-05	7.82148
35	*FAK*	Hs.434281	focal adhesion kinase	8q24	0.00029	7.03583
36	*TRAF6*	Hs.444172	Tumor necrosis factor receptor – associated factor 6	11p13	0.0001	6.71903
37	*MADD*	Hs.82548	MAP-kinase activating death domain	11p11.2	6.30e-05	6.60535
38	*PPP3CB*	Hs.187543	protein phosphatase 3 catalytic subunit, β isoform	10q22.2	0.00012	6.10191
39	*TSC1*	Hs.69429	tuberous sclerosis 1	9q34.13	0.00039	5.92062
40	*STAT5A*	Hs.437058	signal transducer and activator of transcription 5A	17q11.2	0.00015	5.91317
41	*SOCS5*	Hs.169836	suppressor of cytokine signaling 5	2p21	0.00027	5.88452
42	*PHF16*	Hs.82292	PHD finger protein 16	Xp11.3	0.00054	5.84577
43	*PIK3C3*	Hs.418150	phosphoinositide-3-kinase, class 3	18q12.3	0.00035	5.73027
44	*UNC13B*	Hs.155001	unc-13 homologue B	9p13.3	0.00023	5.70029
45	*MAP3K7*	Hs.290346	MAP kinase kinase 7	6q15	0.00045	5.49991
46	*LTBP1*	Hs.241257	latent TGF-β binding protein 1	2p22.3	0.0008	5.38788
47	*ITGA9*	Hs.222	integrin, 9	3p22.3	0.00033	5.35081
48	*GNAQ*	Hs.469951	guanine nucleotide binding protein (G protein), q polypeptide	2q21.1	0.00066	5.30905
49	*MYST3*	Hs.93231	MYST histone acetyltransferase (monocytic leukemia) 3	8p11.21	0.00044	5.16659
50	*SKIP*	Hs.178347	skeletal muscle and kidney enriched inositol phosphatase	17p13.3	0.00052	5.13827
51	*C5*	Hs.1281	complement component 5	9q33.2	0.00092	4.97948
52	*PPP1R15A*	Hs.76556	protein phosphatase 1, regulatory (inhibitor) subunit 15A	19q13.33	0.00075	4.81317
Unknown and other function						
53	*LRP3*	Hs.143641	low density lipoprotein receptor-related protein 3	19q12	6.02e-06	10.2416
54	*SLC9A3*	Hs.123044	solute carrier family 9 (sodium/hydrogen exchanger), isoform 3	5p15.33	0.0002	6.85467
55	*HSU79266*	Hs.23642	protein predicted by clone 23627	11q13.1	0.00037	6.59899
56	*MCART1*	Hs.46791	mitochondrial carrier triple repeat 1	9p13.3	0.00014	6.03726
57	*SEMA5A*	Hs.528707	sema domain, seven thrombospondin repeats (type 1 and type 1-like), transmembrane domain, and short cytoplasmic domain (semaphorin) 5A	5p15.31	0.00027	5.69344
58	*ELN*	Hs.252418	elastin	7q11.23	0.00025	5.53682
59	*KIAA0663*	Hs.17969	KIAA0663 gene product	1q32.1	0.0003	5.45804
60	*OGT*	Hs.405410	*O*-linked *N*-acetylglucosamine (GlcNAc) transferase	Xq13.1	0.00035	5.29243
61	*KIAA0261*	Hs.439188	KIAA0261	10q23.2	0.00041	5.26712
62	*UAP1*	Hs.21293	UDP-N-acteylglucosamine pyrophosphorylase 1	1q24.2	0.00049	5.22761
63	*INPP5E*	Hs.25156	inositol polyphosphate-5-phosphatase, 72 kDa	9q34.3	0.00039	5.22321
64	*HECA*	Hs.6679	headcase homologue (*Drosophila*)	6q24.1	0.00095	5.16452
65	*RPS21*	Hs.372960	ribosomal protein S21	20q13.33	0.00071	5.03318
66	*PCSK7*	Hs.443752	proprotein convertase subtilisin/kexin type 7	11q23.2	0.0006	4.94516
67	*SEC23B*	Hs.173497	Sec23 homologue B	20p11.23	0.00063	4.92033
68	*MGEA5*	Hs.5734	meningioma expressed antigen 5	10q24.32	0.00096	4.79081
69	*C6orf93*	Hs.33944	chromosome 6 open reading frame 93	6q24.2	0.00095	4.73743
70	*HAGH*	Hs.155482	hydroxyacylglutathione hydrolase	16p13.3	0.00082	4.72254
71	*LAMP2*	Hs.232432	lysosomal-associated membrane protein 2	Xq24	0.00086	4.69221

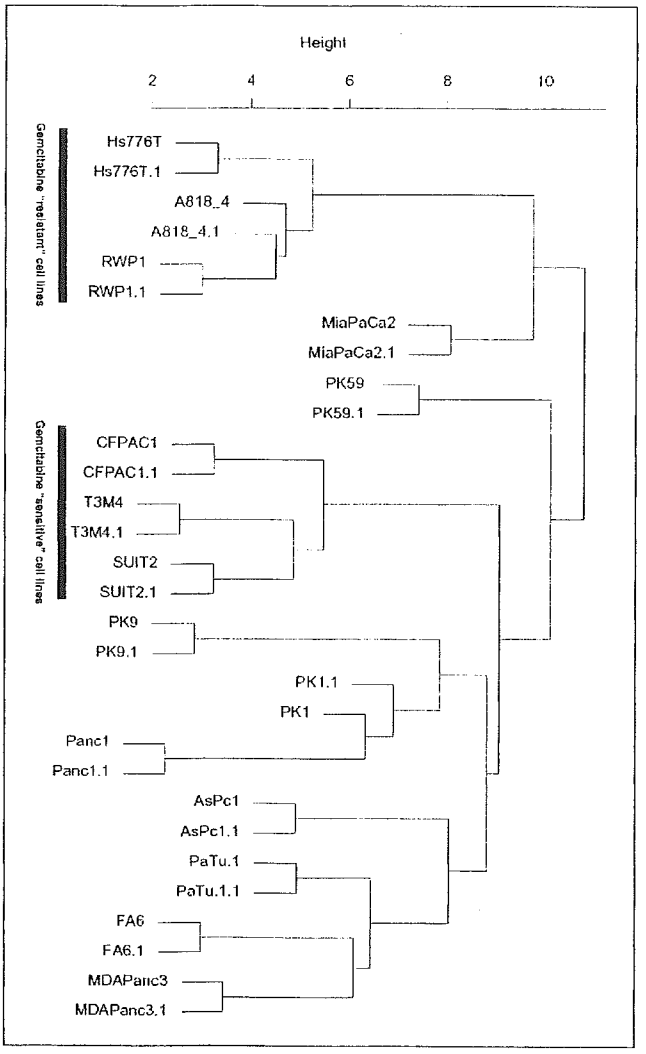

Fig. 2. Dendrogram of hierarchical clustering. The dendrogram shows that gemcitabine-sensitive cell lines CFPAC-1, Suit-2, and T3M4 reside on a separate branch from the gemcitabine-resistant cell lines Hs766T, A818.4, and RWP-1.

done on the gemcitabine-sensitive CFPAC-1 pancreatic cancer cell line. The ability of BNIP3 siRNA to suppress BNIP3 expression was confirmed by both quantitative real-time RT-PCR (Fig. 4A) and Western blot (Fig. 4B). After transfection with BNIP3 siRNA, up to 80% suppression of BNIP3 expression was observed. CFPAC-1 cells treated with BNIP3 siRNA also showed an increase in drug resistance with the IC_{50} rising from 0.5 to 1.2 ng/mL. In comparison, CFPAC-1 cells treated with siRNA targeted against lamin and non-silencing control siRNA showed no change in sensitivity to gemcitabine (Fig. 4C).

Discussion

In the current study we were able to identify a number of genes which are potentially involved in intrinsic resistance to gemcitabine in pancreatic cancer cell lines. Some of these are involved in signaling pathways known from other investigations to contribute to drug resistance (e.g., FAK), whereas in the list of 71 differentially expressed genes, more than half were related to nucleoside metabolism, proliferation, cell cycle regulation, and apoptosis.

The PI3K signaling cascade plays a crucial role in the regulation of apoptosis, acting in part via its downstream target Akt in several cancer cell types including pancreatic cancer (28–30). Activated Akt plays a role in apoptosis suppression by regulating critical factors such as Bcl-associated death promoter, caspase-9, and mammalian target of rapamycin (31). Several studies have already described the contribution of the PI3K/Akt pathway to gemcitabine sensitivity in pancreatic cancer cells. FAK and c-Src play a role in adhesion-dependent activation of the PI3K/Akt pathway and their suppression enhances gemcitabine chemosensitivity in pancreatic cancer (16–18). Moreover, hypoxic conditions also activate the PI3K/Akt pathway in pancreatic cancer (19). In the current study, we identified 71 genes associated with differential gemcitabine sensitivity and, of these, seven encode proteins that contribute to the PI3K/Akt pathway. As well as FAK, of which contribution to drug resistance is well known, integrin α4 may have the ability to stimulate PI3K through PXN as substrate (32, 33). TSC1 and p70S6K are downstream targets of Akt, and PIK3C3 is a member of the PI3K family (34). IGFBP7 can reduce PI3K signaling by binding to IGF and preventing its interaction with its membrane receptor. Two genes that are relatively underexpressed in gemcitabine-resistant cell lines are *p70S6K* and *PXN*. Interestingly, in a leukemia cell clone resistant to apoptosis, although p70S6K activation was increased by signaling through the PI3K/Akt pathway, its selective inhibition did not restore sensitivity to

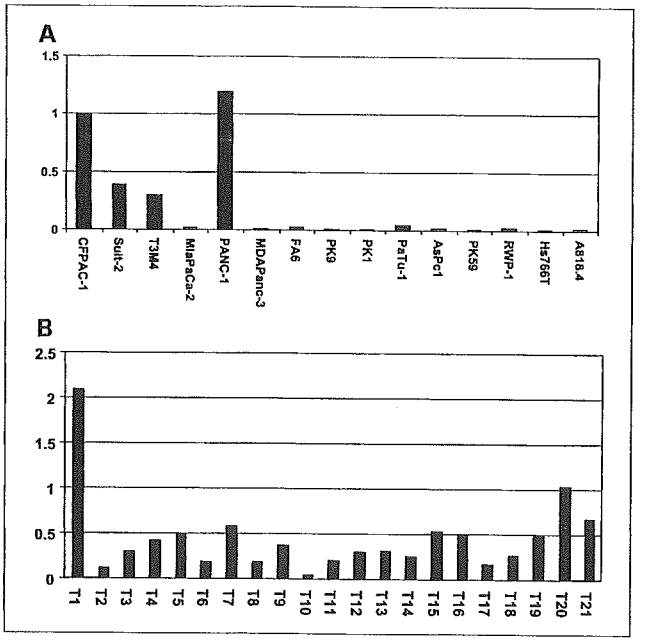

Fig. 3. *A*, BNIP3 expression in pancreatic cancer cell lines determined by quantitative real-time RT-PCR. BNIP3 expression is observed in the gemcitabine-sensitive cancer cell lines CFPAC-1, Suit-2, and T3M4 and only in PANC-1 among the intermediate sensitive group. None of the resistant cell lines express significant levels of this gene product. *B*, BNIP3 expression in pancreatic cancer tissues. Quantitative real-time PCR shows that in 19 of 22 cases BNIP3 expression was down-regulated.

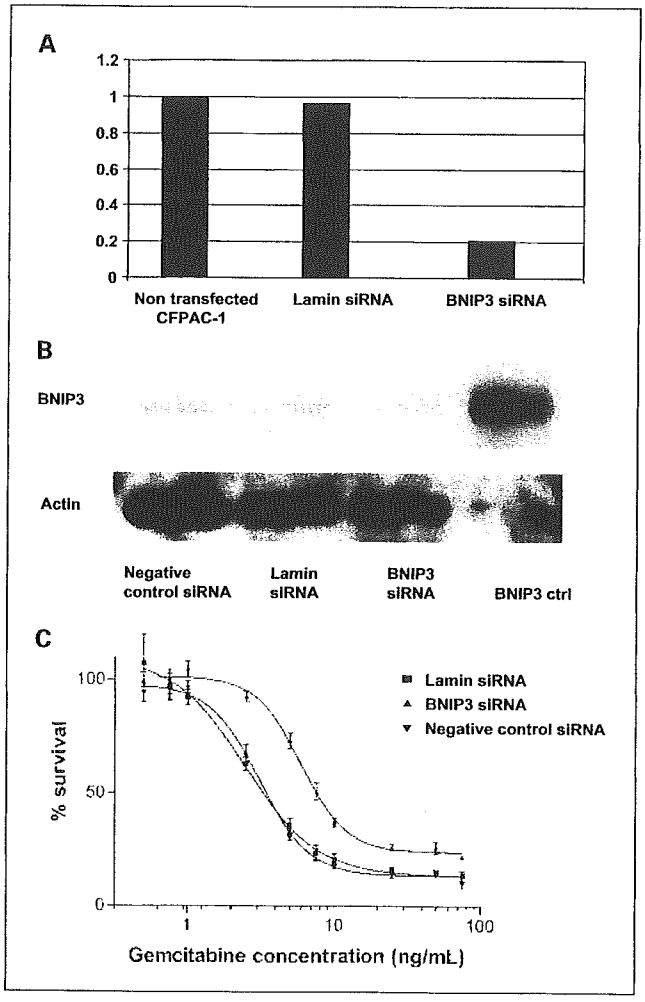

Fig. 4. *A*, representative quantitative real-time RT-PCR data for BNIP3 expression in CFPAC-1 pancreatic cancer cells at 96 hours following treatment with BNIP3 siRNA or lamin siRNA. *B*, Western blot for BNIP3 96 hours following treatment with nonsilencing negative control siRNA, lamin siRNA, and BNIP3 siRNA. Protein lysate extracted from BNIP3-transfected 293 cells was used for positive control. Neither control nor lamin siRNA significantly affected BNIP3 expression, whereas BNIP3 siRNA induced marked (up to 80%) suppression of BNIP3. *C*, dose-response curves for gemcitabine in the CFPAC-1 pancreatic cancer cell line treated with siRNA. ▼, CFPAC-1 treated with control siRNA; ■, CFPAC-1 treated with lamin siRNA; and ▲, CFPAC-1 treated with BNIP3 siRNA. CFPAC-1 treated with BNIP3 siRNA shows an increase in resistance to gemcitabine.

drugs (28). PXN is a substrate for FAK and SRC, whereas negative regulators of these also bind directly to it (35). Altogether, these results strongly support the importance of the PI3K/Akt pathway in gemcitabine sensitivity in pancreatic cancer.

The TGF-β pathway has also been reported to be involved in sensitivity to cisplatin chemotherapy in a leukemia model. Stimulation of TGF-β receptors leads to activation of Smad proteins that cause growth inhibition and induce apoptosis in normal cells. Several pancreatic cancer cell lines are resistant to TGF-β–induced growth arrest (36) and that might be another reason why pancreatic cancer is resistant to chemotherapeutic reagents. In our gene list, *RALBP1*, *SMAD2*, and *LTBP1* are all members of the TGF-β signaling pathway expressed in resistant cell lines and can also potentially contribute to gemcitabine sensitivity.

Interestingly, among our selected genes, several are located at the same chromosomal regions and these loci are also previously reported as frequent sites for aberrations and amplification in pancreatic cancer (25–27). This could be a possible reason for differential abundance of those gene transcripts in pancreatic cancer cells.

In this study, we identified *BNIP3* as a gene strongly associated with intrinsic resistance to gemcitabine and frequently down-regulated in pancreatic cancer. We also show that suppression of BNIP3 by siRNA reduced gemcitabine-induced cytotoxicity in pancreatic cancer cells *in vitro*. Previously, BNIP3 expression was shown to be down-regulated in clones with acquired resistance against 5-fluorouracil compared with their parental colorectal cancer cell line (37). Another study showed that BNIP3 expression was associated with paclitaxel response in an ovarian cancer model (38).

BNIP3, a member of the BH3-only subfamily of Bcl-2 family proteins, heterodimerizes and antagonizes the activity of prosurvival proteins such as Bcl-2 and Bcl-xl, thus promoting apoptosis. Overexpression of BNIP3 induces cell death characterized by its localization at the mitochondria, by opening of the permeability transition pore, and by loss of membrane potential and production of reactive oxygen species (39, 40).

BNIP3 expression is normally undetectable in most tissues, but it has been reported to be expressed in hypoxic regions (41, 42) and can be induced in cell lines by hypoxia *in vitro* (43). Despite the fact that pancreatic cancer usually grows under hypoxic conditions (44, 45), our study shows that BNIP3 expression levels in both cell lines and tissues from surgically resected specimens are low. Furthermore, we have determined that hypoxia does not induce expression of BNIP3 in cell lines that are intrinsically resistant to gemcitabine (supplementary data available at http://sci.cancerresearchuk.org/axp/mphh/ccr04/). Recently, Okami et al. (46) clearly showed a high prevalence of BNIP3 down-regulation in pancreatic cancer and showed that it is caused by methylation of its promoter site.

In our study of a large series of clinical specimens and cell lines, we were able to show that only a small proportion of cases continue to express BNIP3 at normal levels (those observed in normal pancreas which is composed predominantly of acinar tissue). It will be interesting to integrate analysis of BNIP3 status in biomarker studies for clinical trials of chemotherapeutic agents in pancreatic cancer, where responses are typically observed in a similarly small proportion of cases (47).

In conclusion, we have highlighted the potential importance of the PI3K/Akt pathway in gemcitabine resistance and have shown the effect of BNIP3 on gemcitabine sensitivity in a pancreatic cancer cell line model. This is the first report that targeting BNIP3 could increase tumor cell susceptibility to such a chemotherapeutic agent. BNIP3 could therefore be a promising candidate marker for gemcitabine chemosensitivity, and determining BNIP3 status could potentially aid in decision-making when treating patients with pancreatic adenocarcinoma, as well as representing a potential gene therapeutic target to increase gemcitabine sensitivity.

References

1. Jemal A, Murray T, Samuels A, Ghafoor A, Ward E, Thun MJ. Cancer statistics, 2003. CA Cancer J Clin 2003;53:5–26.
2. Casper ES, Green MR, Kelsen DP, et al. Phase II trial of gemcitabine (2,2′-difluorodeoxycytidine) in patients with adenocarcinoma of the pancreas. Invest New Drugs 1994;12:29–34.
3. Rothenberg ML, Moore MJ, Cripps MC, et al. A phase II trial of gemcitabine in patients with 5-FU-refractory pancreas cancer. Ann Oncol 1996;7:347–53.
4. Burris HA, Moore MJ, Andersen J, et al. Improvements in survival and clinical benefit with gemcitabine as first-line therapy for patients with advanced pancreas cancer: a randomized trial. J Clin Oncol 1997;15: 2403–13.
5. Rauchwerger DR, Firby PS, Hedley DW, Moore MJ. Equilibrative-sensitive nucleoside transporter and its role in gemcitabine sensitivity. Cancer Res 2000;60: 6075–9.
6. Mackey JR, Mani RS, Selner M, et al. Functional nucleoside transporters are required for gemcitabine influx and manifestation of toxicity in cancer cell lines. Cancer Res 1998;58:4349–57.
7. Dumontet C, Bauchu EC, Fabianowska K, et al. Common resistance mechanisms to nucleoside analogues in variants of the human erythroleukemic line K562. Adv Exp Med Biol 1999;457:571–7.
8. Goan YG, Zhou B, Hu E, Mi S, Yen Y. Overexpression of ribonucleotide reductase as a mechanism of resistance to 2,2-difluorodeoxycytidine in the human KB cancer cell line. Cancer Res 1999;59:4204–7.
9. Liu X, Zhou B, Xue L, et al. Nuclear factor Y regulation and promoter transactivation of human ribonucleotide reductase subunit M2 gene in a gemcitabine resistant KB clone. Biochem Pharmacol 2004;67:1499–511.
10. Davidson JD, Ma L, Flagella M, Geeganage S, Gelbert LM, Slapak CA. An increase in the expression of ribonucleotide reductase large subunit 1 is associated with gemcitabine resistance in non-small cell lung cancer cell lines. Cancer Res 2004;64: 3761–6.
11. Duxbury MS, Ito H, Zinner MJ, Ashley SW, Whang EE. RNA interference targeting the M2 subunit of ribonucleotide reductase enhances pancreatic adenocarcinoma chemosensitivity to gemcitabine. Oncogene 2004;23:1539–48.
12. Galmarini CM, Clarke ML, Jordheim L, et al. Resistance to gemcitabine in a human follicular lymphoma cell line is due to partial deletion of the deoxycytidine kinase gene. BMC Pharmacol 2004;4:8.
13. Galmarini CM, Clarke ML, Falette N, Puisieux A, Mackey JR, Dumontet C. Expression of a non-functional p53 affects the sensitivity of cancer cells to gemcitabine. Int J Cancer 2002;97:439–45.
14. Shi X, Liu S, Kleeff J, Friess H, Buchler MW. Acquired resistance of pancreatic cancer cells towards 5-fluorouracil and gemcitabine is associated with altered expression of apoptosis-regulating genes. Oncology 2002;62:354–62.
15. Schniewind B, Christgen M, Kurdow R, et al. Resistance of pancreatic cancer to gemcitabine treatment is dependent on mitochondria-mediated apoptosis. Int J Cancer 2004;109:182–8.
16. Duxbury MS, Ito H, Zinner MJ, Ashley SW, Whang EE. Inhibition of SRC tyrosine kinase impairs inherent and acquired gemcitabine resistance in human pancreatic adenocarcinoma cells. Clin Cancer Res 2004; 10:2307–18.
17. Duxbury MS, Ito H, Zinner MJ, Ashley SW, Whang EE. siRNA directed against c-Src enhances pancreatic adenocarcinoma cell gemcitabine chemosensitivity. J Am Coll Surg 2004;198:953–9.
18. Duxbury MS, Ito H, Zinner MJ, Ashley SW, Whang EE. Focal adhesion kinase gene silencing promotes anoikis and suppresses metastasis of human pancreatic adenocarcinoma cells. Surgery 2004;135:555–62.
19. Yokoi K, Fidler IJ. Hypoxia increases resistance of human pancreatic cancer cells to apoptosis induced by gemcitabine. Clin Cancer Res 2004;10: 299–2306.
20. Kobari M, Matsuno S, Sato T, Kan M, Tachibana T. Establishment of a human pancreatic cancer cell line and detection of pancreatic cancer associated antigen. Tohoku J Exp Med 1984;143:33–46.
21. Furukawa T, Duguid WP, Rosenberg L, Viallet J, Galloway DA, Tsao MS. Long-term culture and immortalization of epithelial cells from normal adult human pancreatic ducts transfected by the E6E7 gene of human papilloma virus 16. Am J Pathol 1996;148: 1763–70.
22. Terris B, Blaveri E, Crnogorac-Jurcevic T, et al. Characterization of gene expression profiles in intraductal papillary-mucinous tumors of the pancreas. Am J Pathol 2002;160:1745–54.
23. Huber W, von Heydebreck A, Sultmann H, Poustka A, Vingron M. Variance stabilization applied to microarray data calibration and to the quantification of differential expression. Bioinformatics 2002;18 Suppl 1:S96–104.
24. Benjamini Y, Drai D, Elmer G, Kafkafi N, Golani I. Controlling the false discovery rate in behavior genetics research. Behav Brain Res 2001;125:279–84.
25. Iacobuzio-Donahue CA, van der Heijden MS, Baumgartner MR, et al. Large-scale allelotype of pancreaticobiliary carcinoma provides quantitative estimates of genome-wide allelic loss. Cancer Res 2004;64:871–5.
26. Schleger C, Arens N, Zentgraf H, Bleyl U, Verbeke C. Identification of frequent chromosomal aberrations in ductal adenocarcinoma of the pancreas by comparative genomic hybridization (CGH). J Pathol 2000;191: 27–32.
27. Ghadimi BM, Schrock E, Walker RL, et al. Specific chromosomal aberrations and amplification of the AIB1 nuclear receptor coactivator gene in pancreatic carcinomas. Am J Pathol 1999;154: 525–36.
28. Neri LM, Borgatti P, Tazzari PL, et al. The phosphoinositide 3-kinase/AKT1 pathway involvement in drug and all-*trans*-retinoic acid resistance of leukemia cells. Mol Cancer Res 2003;1:234–46.
29. Franke TF, Hornik CP, Segev L, Shostak GA, Sugimoto C. PI3K/Akt and apoptosis: size matters. Oncogene 2003;22:8983–98.
30. Seufferlein T. Novel protein kinases in pancreatic cell growth and cancer. Int J Gastrointest Cancer 2002;31: 15–21.
31. Asnaghi L, Calastretti A, Bevilacqua A, et al. Bcl-2 phosphorylation and apoptosis activated by damaged microtubules require mTOR and are regulated by Akt. Oncogene 2004;23:5781–91.
32. Turner CE. Paxillin and focal adhesion signalling. Nat Cell Biol 2000;2:E231–6.
33. Schaller MD. FAK and paxillin: regulators of N-cadherin adhesion and inhibitors of cell migration? J Cell Biol 2004;166:157–9.
34. Stopkova P, Saito T, Papolos DF, et al. Identification of PIK3C3 promoter variant associated with bipolar disorder and schizophrenia. Biol Psychiatry 2004;55:981–8.
35. Turner CE. Paxillin interactions. J Cell Sci 2000;113 Pt 23:4139–40.
36. Nicolas FJ, Hill CS. Attenuation of the TGF-β-Smad signaling pathway in pancreatic tumor cells confers resistance to TGF-β-induced growth arrest. Oncogene 2003;22:3698–711.
37. de Angelis PM, Fjell B, Kravik KL, et al. Molecular characterizations of derivatives of HCT116 colorectal cancer cells that are resistant to the chemotherapeutic agent 5-fluorouracil. Int J Oncol 2004;24:1279–88.
38. Bani MR, Nicoletti MI, Alkharouf NW, et al. Gene expression correlating with response to paclitaxel in ovarian carcinoma xenografts. Mol Cancer Ther 2004;3:111–21.
39. Ray R, Chen G, Vande Velde C, et al. BNIP3 heterodimerizes with Bcl-2/Bcl-X(L) and induces cell death independent of a Bcl-2 homology 3 (BH3) domain at both mitochondrial and nonmitochondrial sites. J Biol Chem 2000;275:1439–48.
40. Vande Velde C, Cizeau J, Dubik D, et al. BNIP3 and genetic control of necrosis-like cell death through the mitochondrial permeability transition pore. Mol Cell Biol 2000;20:5454–68.
41. Sowter HM, Ferguson M, Pym C, et al. Expression of the cell death genes BNip3 and NIX in ductal carcinoma *in situ* of the breast; correlation of BNip3 levels with necrosis and grade. J Pathol 2003;201:573–80.
42. Kubasiak LA, Hernandez OM, Bishopric NH, Webster KA. Hypoxia and acidosis activate cardiac myocyte death through the Bcl-2 family protein BNIP3. Proc Natl Acad Sci U S A 2002;99: 12825–30.
43. Bruick RK. Expression of the gene encoding the proapoptotic Nip3 protein is induced by hypoxia. Proc Natl Acad Sci U S A 2000;97:9082–7.
44. Koong AC, Mehta VK, Le QT, et al. Pancreatic tumors show high levels of hypoxia. Int J Radiat Oncol Biol Phys 2000;48:919–22.
45. Duffy JP, Eibl G, Reber HA, Hines OJ. Influence of hypoxia and neoangiogenesis on the growth of pancreatic cancer. Mol Cancer 2003;2:12.
46. Okami J, Simeone DM, Logsdon CD. Silencing of the hypoxia-inducible cell death protein BNIP3 in pancreatic cancer. Cancer Res 2004;64:5338–46.
47. Neoptolemos JP, Stocken DD, Friess H, et al. A randomized trial of chemoradiotherapy and chemotherapy after resection of pancreatic cancer. N Engl J Med 2004;350:1200–10.